

1 **Erosion of somatic tissue identity with loss of the X-linked**
2 **intellectual disability factor KDM5C**

3

4 Katherine M. Bonefas, Ilakkiya Venkatachalam, and Shigeki Iwase.

5 **Abstract**

6 Mutations in numerous chromatin-modifying enzymes cause neurodevelopmental disorders (NDDs) with
7 unknown mechanisms. Loss of repressive chromatin regulators can lead to the aberrant transcription of
8 tissue-specific genes outside of their intended context, however the mechanisms and consequences of
9 their dysregulation are largely unknown. Here, we examine the role of lysine demethylase 5c (KDM5C),
10 an eraser of histone 3 lysine 4 di and tri-methylation (H3K4me2/3) mutated in Claes-Jensen X-linked
11 intellectual disability, in tissue identity. We found male *Kdm5c* knockout (-KO) mice, which recapitulate
12 key human neurological phenotypes, aberrantly expresses many liver, muscle, ovary, and testis genes
13 within the amygdala and hippocampus. Gonad-enriched genes misexpressed in the *Kdm5c*-KO brain are
14 unique to germ cells, indicating an erosion of the soma-germline boundary. Germline genes are typically
15 decommissioned in somatic lineages in the post-implantation epiblast, yet *Kdm5c*-KO epiblast-like cells
16 (EpiLCs) aberrantly expressed key regulators of germline identity and meiosis, including *Dazl* and *Stra8*.
17 Germline gene suppression is sexually dimorphic, as female EpiLCs required a higher dose of KDM5C
18 to maintain germline gene suppression. Using a comprehensive list of mouse germline-enriched genes,
19 we found KDM5C is selectively recruited to a subset of germline gene promoters that contain CpG islands
20 (CGIs) to facilitate DNA CpG methylation (CpGme) during ESC to EpiLC differentiation. However, late stage
21 spermatogenesis genes devoid of promoter CGIs can also become activated in *Kdm5c*-KO cells via ectopic
22 activation by RFX transcription factors. Thus, distinct mechanisms govern the misexpression of germline
23 gene classes, including activation by ectopic germline programs that mirror germ cell development within
24 somatic tissues.

25 **Introduction**

26 A single genome holds the instructions to generate the myriad of cell types found within an organism.
27 This is, in part, accomplished by chromatin regulators that can either promote or impede lineage-specific

28 gene expression through DNA and histone modifications^{1–5}. Human genetic studies revealed mutations in
29 chromatin regulators are a major cause of neurodevelopmental disorders (NDDs)⁶ and many studies have
30 identified their importance for regulating brain-specific transcriptional programs. Loss of some chromatin
31 regulators can also result in the ectopic expression of tissue-specific genes outside of their target environment,
32 such as the misexpression of liver-specific genes within adult neurons⁷. However, the mechanisms underlying
33 ectopic gene expression and its impact upon neurodevelopment are poorly understood.

34 To elucidate the role of tissue identity in chromatin-linked NDDs, it is essential to first characterize the
35 nature of the dysregulated genes and the molecular mechanisms governing their de-repression. Here we
36 focus on lysine demethylase 5C (KDM5C, also known as SMCX or JARID1C), which erases histone 3 lysine
37 4 di- and trimethylation (H3K4me2/3), a permissive chromatin modification enriched at gene promoters⁸.
38 Pathogenic mutations in *KDM5C* cause Intellectual Developmental Disorder, X-linked, Syndromic, Claes-
39 Jensen Type (MRXSCJ, OMIM: 300534). MRXSCJ is more common and severe in males and its neurological
40 phenotypes include intellectual disability, seizures, aberrant aggression, and autistic behaviors^{9–11}. Male
41 *Kdm5c* knockout (-KO) mice recapitulate key MRXSCJ phenotypes, including hyperaggression, increased
42 seizure propensity, and learning impairments^{12,13}. RNA sequencing (RNA-seq) of the *Kdm5c*-KO hippocam-
43 pus revealed ectopic expression of some germline genes within the brain¹³. However, it is unclear if other
44 tissue-specific genes are aberrantly transcribed with KDM5C loss, at what point in development germline
45 gene misexpression begins, and what mechanisms underlie their dysregulation.

46 Distinguishing between germ cells and somatic cells is a key feature of multicellularity¹⁴ that occurs
47 during early embryogenesis in many metazoans¹⁵. In mammals, chromatin regulators are crucial for
48 decommissioning germline genes during the transition from naïve to primed pluripotency. Initially, germline
49 gene promoters gain repressive histone H2A lysine 119 monoubiquitination (H2AK119ub1)¹⁶ and histone 3
50 lysine 9 trimethylation (H3K9me3)^{16,17} in embryonic stem cells (ESCs) and are then decorated with DNA
51 CpG methylation (CpGme) in the post-implantation embryo^{17–20}. The contribution of KDM5C to this process
52 remains unclear. Furthermore, studies on germline gene repression have primarily been conducted in
53 males and focused on marker genes important for germ cell development rather than germline genes as a
54 whole, given the lack of a curated germline-enriched gene list. Therefore, it is unknown if the mechanism
55 of repression differs between sexes or for certain classes of germline genes, e.g. meiotic genes versus
56 spermatid differentiation genes.

57 To illuminate KDM5C's role in tissue identity, here we characterized the aberrant expression of tissue-
58 enriched genes within the *Kdm5c*-KO brain and epiblast-like stem cells (EpiLCs), an *in vitro* model of the
59 post-implantation embryo. We curated a list of mouse germline-enriched genes, which enabled genome-wide
60 analysis of germline gene silencing mechanisms for the first time. Based on the data presented below, we
61 propose KDM5C plays a fundamental, sexually dimorphic role in the development of tissue identity during
62 early embryogenesis, including the establishment of the soma-germline boundary.

63 **Results**

64 **Tissue-enriched genes are aberrantly expressed in the *Kdm5c*-KO brain**

65 Previous RNA sequencing (RNA-seq) of the adult male *Kdm5c*-KO hippocampus revealed ectopic
66 expression of some germline genes unique to the testis¹³. It is currently unknown if the testis is the only
67 tissue type misexpressed in the *Kdm5c*-KO brain. We thus systematically tested whether other tissue-specific
68 genes are misexpressed in the male brain with constitutive knockout of *Kdm5c* (*Kdm5c*^{-y}, 5CKO)²¹ by using
69 a published list of mouse tissue-enriched genes²².

70 We found a large proportion of significantly upregulated genes (DESeq2²³, log2 fold change > 0.5,
71 q < 0.1) within the male *Kdm5c*-KO amygdala and hippocampus are typically enriched within non-brain
72 tissues (Amygdala: 35%, Hippocampus: 24%) (Figure 1A-B). For both the amygdala and hippocampus,
73 the majority of tissue-enriched differentially expressed genes (DEGs) were testis genes (Figure 1A-B).
74 Even though the testis has the largest total number of tissue-biased genes (2,496 genes) compared to any
75 other tissue, testis-biased DEGs were significantly enriched for both brain regions (Amygdala p = 1.83e-05,
76 Odds Ratio = 5.13; Hippocampus p = 4.26e-11, Odds Ratio = 4.45, Fisher's Exact Test). An example of a
77 testis-enriched gene misexpressed in the *Kdm5c*-KO brain is *FK506 binding protein 6* (*Fkbp6*), a known
78 regulator of PIWI-interacting RNAs (piRNAs) and meiosis^{24,25} (Figure 1C).

79 Interestingly, we also observed significant enrichment of ovary-biased DEGs in both the amygdala and
80 hippocampus (Amygdala p = 0.00574, Odds Ratio = 18.7; Hippocampus p = 0.048, Odds Ratio = 5.88,
81 Fisher's Exact) (Figure 1A-B). Ovary-enriched DEGs included *Zygotic arrest 1* (*Zar1*), which sequesters
82 mRNAs in oocytes for meiotic maturation²⁶ (Figure 1D). Given that the *Kdm5c*-KO mice we analyzed are
83 male, these data demonstrate that the ectopic expression of gonad-enriched genes is independent of
84 organismal sex.

85 Although not consistent across brain regions, we also found significant enrichment of DEGs biased
86 towards two non-gonadal tissues - the liver (Amygdala p = 0.04, Odds Ratio = 6.58, Fisher's Exact Test) and
87 muscles (Hippocampus p = 0.01, Odds Ratio = 6.95, Fisher's Exact Test) (Figure 1A-B). *Apolipoprotein C-I*
88 (*Apoc1*) a lipoprotein metabolism and transport gene, is among the liver-biased DEG derepressed in both
89 the hippocampus and amygdala²⁷ and its brain overexpression has been implicated in Alzheimer's disease²⁸
90 (Figure 1E).

91 For all *Kdm5c*-KO tissue-enriched DEGs, aberrantly expressed mRNAs are polyadenylated and spliced
92 into mature transcripts (Figure 1C-E). Of note, we observed little to no dysregulation of brain-enriched genes
93 (Amygdala p = 1, Odds Ratio = 1.22; Hippocampus p = 0.74, Odds Ratio = 1.22, Fisher's Exact), despite the
94 fact these are brain samples and the brain has the second highest total number of tissue-enriched genes
95 (708 genes). Altogether, these results suggest the aberrant expression of tissue-enriched genes within the
96 brain is a major effect of KDM5C loss.

97 **Germline genes are misexpressed in the *Kdm5c*-KO brain**

98 *Kdm5c*-KO brain expresses testicular germline genes¹³, however the testis also contains somatic cells that
99 support hormone production and germline functions. To determine if *Kdm5c*-KO results in ectopic expression
100 of somatic testicular genes, we first evaluated the known functions of testicular DEGs through gene ontology.
101 We found *Kdm5c*-KO testis-enriched DEGs had high enrichment of germline-relevant ontologies, including
102 spermatid development (GO: 0007286, p.adjust = 6.2e-12) and sperm axoneme assembly (GO: 0007288,
103 p.adjust = 2.45e-14) (Figure 2A).

104 We then evaluated testicular DEG expression in wild-type testes versus testes with germ cell depletion²⁹,
105 which was accomplished by heterozygous *W* and *Wv* mutations in the enzymatic domain of *c-Kit* (*Kit*^{W/Wv})³⁰.
106 Almost all *Kdm5c*-KO testis-enriched DEGs lost expression with germ cell depletion (Figure 2B). We then
107 assessed testis-enriched DEG expression in a published single cell RNA-seq dataset that identified cell
108 type-specific markers within the testis³¹. Some *Kdm5c*-KO testis-enriched DEGs were classified as specific
109 markers for different germ cell developmental stages (e.g. spermatogonia, spermatocytes, round spermatids,
110 and elongating spermatids), yet none marked somatic cells (Figure 2C). Together, these data demonstrate
111 that the *Kdm5c*-KO brain aberrantly expresses germline genes but not somatic testicular genes, reflecting an
112 erosion of the soma-germline boundary.

113 As of yet, research on germline gene silencing mechanisms has focused on a handful of key genes rather
114 than assessing germline gene suppression genome-wide, due to the lack of a comprehensive gene list.
115 We therefore generated a list of mouse germline-enriched genes using RNA-seq datasets of *Kit*^{W/Wv} mice
116 that included males and females at embryonic day 12, 14, and 16³² and adult male testes²⁹. We defined
117 genes as germline-enriched if their expression met the following criteria: 1) their expression is greater than
118 1 FPKM in wild-type gonads 2) their expression in any non-gonadal tissue of adult wild type mice²² does
119 not exceed 20% of their maximum expression in the wild-type germline, and 3) their expression in the germ
120 cell-depleted gonads, for any sex or time point, does not exceed 20% of their maximum expression in the
121 wild-type germline. These criteria yielded 1,288 germline-enriched genes (Figure 2D), which was hereafter
122 used as a resource to globally characterize germline gene misexpression with *Kdm5c* loss (Supplementary
123 table 1).

124 ***Kdm5c*-KO epiblast-like cells aberrantly express key regulators of germline identity**

125 Germ cells are typically distinguished from somatic cells soon after the embryo implants into the uterine
126 wall^{33,34}, when germline genes are silenced in epiblast stem cells that will form the somatic tissues³⁵. This
127 developmental time point can be modeled *in vitro* through differentiation of naïve embryonic stem cells
128 (nESCs) into epiblast-like stem cells (EpiLCs) (Figure 3A)^{36,37}. While some germline-enriched genes are
129 also expressed in nESCs and in the 2-cell stage^{38–40}, they are silenced as they differentiate into EpiLCs^{17,18}.
130 Therefore, we tested if KDM5C was necessary for the initial silencing of germline genes in somatic lineages

131 by evaluating the impact of *Kdm5c* loss in male EpiLCs.
132 *Kdm5c*-KO cell morpholgy during ESC to EpiLC differentiation appeared normal (Figure 3B) and EpiLCs
133 properly expressed markers of primed pluripotency, such as *Dnmt3b*, *Fgf5*, *Pou3f1*, and *Otx2* (Figure 3C). We
134 then identified tissue-enriched DEGs in a RNA-seq dataset of wild-type and *Kdm5c*-KO EpiLCs⁴¹ (DESeq2,
135 log2 fold change > 0.5, q < 0.1). Similar to the *Kdm5c*-KO brain, we observed general dysregulation of
136 tissue-enriched genes, with the largest number of genes belonging to the brain and testis, although they
137 were not significantly enriched (Figure 3D). Using our list of mouse germline-enriched genes assembled
138 above, we found 68 germline genes were misexpressed in male *Kdm5c*-KO EpiLCs.

139 We then compared EpiLC germline DEGs to those expressed in the *Kdm5c*-KO brain to determine if
140 germline genes are constitutively dysregulated or change over the course of development. The majority of
141 germline DEGs were unique to either EpiLCs or the brain, with only *D1Pas1* and *Cyct* shared across all
142 tissue/cell types (Figure 3E-F). EpiLC germline DEGs had particularly high enrichment of meiosis-related
143 gene ontologies when compared to the brain (Figure 3G), such as meiotic cell cycle process (GO:1903046,
144 p.adjust = 2.2e-07) and meiotic nuclear division (GO:0140013, p.adjust = 1.37e-07). While there was
145 modest enrichment of meiotic gene ontologies in both brain regions, the *Kdm5c*-KO hippocampus primarily
146 expressed late-stage spermatogenesis genes involved in sperm axoneme assembly (GO:0007288, p.adjust
147 = 0.00621) and sperm motility (GO:0097722, p.adjust = 0.00612).

148 Notably, DEGs unique to *Kdm5c*-KO EpiLCs included key drivers of germline identity, such as *Stimulated*
149 *by retinoic acid 8* (*Stra8*: log2 fold change = 3.73, q = 2.17e-39) and *Deleted in azoospermia like* (*Dazl*):
150 log2 fold change = 3.36, q = 3.19e-12) (Figure 3H). These genes are typically expressed when primordial
151 germ cells (PGCs) are committed to the germline fate and later in life to trigger meiotic gene expression
152 programs⁴²⁻⁴⁴. Of note, some germline genes, including *Dazl*, are also expressed in the two-cell embryo^{39,45}.
153 However, we did not see derepression of two-cell stage-specific genes, like *Duxf3* (*Dux*) (log2 fold change
154 = -0.282, q = 0.337) and *Zscan4d* (log2 fold change = 0.25, q = 0.381) (Figure 3H), indicating *Kdm5c*-KO
155 EpiLCs do not revert back to a 2-cell state. Altogether, *Kdm5c*-KO EpiLCs express key drivers of germline
156 identity and meiosis while the brain primarily expresses spermiogenesis genes, indicating germline gene
157 misexpression mirrors germline development during the progression of somatic development.

158 **Female epiblast-like cells have increased sensitivity to germline gene misexpression
159 with *Kdm5c* loss**

160 It is currently unknown if the misexpression of germline genes is influenced by sex, as previous studies
161 on germline gene repressors have focused on male cells^{16,17,19,46,47}. Sex is particularly pertinent in the case
162 of KDM5C because it partially escapes X chromosome inactivation (XCI), resulting in a higher dosage in
163 females⁴⁸⁻⁵¹. We therefore explored the impact of chromosomal sex upon germline gene suppression by
164 comparing their dysregulation in male *Kdm5c* hemizygous knockout (XY *Kdm5c*-KO, XY 5CKO), female

165 homozygous knockout (XX *Kdm5c*-KO, XX 5CKO), and female heterozygous knockout (XX *Kdm5c*-HET, XX
166 5CHET) EpiLCs⁴¹.

167 In EpiLCs, homozygous and heterozygous *Kdm5c* knockout females expressed over double the number
168 of germline-enriched genes than hemizygous males (Figure 4A). While the majority of germline DEGs in
169 *Kdm5c*-KO males were also dysregulated in females (74%), many were sex-specific, such as *Tktl2* and *Esx1*
170 (Figure 4B). We then compared the known functions of germline genes dysregulated only in females (XX
171 only - unique to XX *Kdm5c*-KO, XX *Kdm5c*-HET, or both), only in males (XY only), or in all samples (shared)
172 (Figure 4C). Female-specific germline DEGs were enriched for meiotic (GO:0051321 - meiotic cell cycle) and
173 flagellar (GO:0003341 - cilium movement) functions, while male-specific DEGs had roles in mitochondrial
174 and cell signaling (GO:0070585 - protein localization to mitochondrion). Germline transcripts expressed in
175 both sexes were enriched for meiotic (GO:0140013 - meiotic nuclear division) and egg-specific functions
176 (GO:0007292 - female gamete generation).

177 The majority of germline genes expressed in both sexes were more highly dysregulated in females
178 compared to males (Figure 4D-F). This increased degree of dysregulation in females, along with the
179 increased total number of germline genes, indicates females are more sensitive to losing KDM5C-mediated
180 germline gene suppression. Female sensitivity could be due to impaired XCI in *Kdm5c* mutants⁴¹, as many
181 spermatogenesis genes lie on the X chromosome^{52,53}. However, female germline DEGs were not biased
182 towards the X chromosome and had a similar overall proportion of X chromosome DEGs compared to
183 males (XY *Kdm5c*-KO - 10.29%, XX *Kdm5c*-HET - 7.43%, XX *Kdm5c*-KO - 10.59%) (Figure 4G). The
184 majority of germline DEGs instead lie on autosomes for both male and female *Kdm5c* mutants (Figure 4G).
185 Thus, while female EpiLCs are more prone to germline gene misexpression with KDM5C loss, it is likely
186 independent of XCI defects.

187 **Germline gene misexpression in *Kdm5c* mutants is independent of germ cell sex**

188 Although many germline genes have shared functions in the male and female germline, e.g. PGC
189 formation, meiosis, and genome defense, some have unique or sex-biased expression. Therefore, we
190 wondered if *Kdm5c* mutant males would primarily express sperm genes while mutant females would primarily
191 express egg genes. To comprehensively assess whether germline gene sex corresponds with *Kdm5c* mutant
192 sex, we first filtered our list of germline-enriched genes for egg and sperm-biased genes (Figure 4H). We
193 defined germ cell sex-biased genes as those whose expression in the opposite sex, at any time point, is no
194 greater than 20% of the gene's maximum expression in a given sex. This criteria yielded 67 egg-biased,
195 1,024 sperm-biased, and 197 unbiased germline-enriched genes. We found regardless of sex, egg, sperm,
196 and unbiased germline genes were dysregulated in all *Kdm5c* mutants at similar proportions (Figure 4I-J).
197 Furthermore, germline genes dysregulated exclusively in either male or female mutants were also not biased
198 towards their corresponding germ cell sex (Figure 4I). Altogether, these results demonstrate sex differences
199 in germline gene dysregulation is not due to sex-specific activation of sperm or egg transcriptional programs.

200 **KDM5C binds to a subset of germline gene promoters during early embryogenesis**

201 KDM5C binds to the promoters of several germline genes in embryonic stem cells (ESCs) but its binding
202 is absent in neurons^{13,54}. However, the lack of a comprehensive list of germline-enriched genes prohibited
203 genome-wide characterization of KDM5C binding at germline gene promoters. Thus, it is unclear if KDM5C
204 is enriched at germline gene promoters, what types of germline genes KDM5C regulates, and if its binding is
205 maintained at any germline genes in neurons.

206 To address these questions, we analyzed KDM5C chromatin immunoprecipitation followed by DNA
207 sequencing (ChIP-seq) datasets in EpiLCs⁴¹ and primary forebrain neuron cultures (PNCs)¹². EpiLCs had a
208 higher total number of high-confidence KDM5C peaks than PNCs (EpiLCs: 5,808, PNCs: 1,276, MACS2 q <
209 0.1 and fold enrichment > 1). KDM5C was primarily localized to gene promoters in both cell types (Promoters
210 = transcription start site (TSS) ± 500bp, EpiLCs: 4,190, PNCs: 745), although PNCs showed increased
211 localization to non-promoter regions (Figure 5A).

212 The majority of promoters bound by KDM5C in PNCs were also bound in EpiLCs (513 shared promoters),
213 however a large portion of gene promoters were bound by KDM5C only in EpiLCs (3,677 EpiLC only
214 promoters) (Figure 5B). Genes bound by KDM5C in both PNCs and EpiLCs were enriched for functions
215 involving nucleic acid turnover, such as deoxyribonucleotide metabolic process (GO:0009262, p.adjust =
216 8.28e-05) (Figure 5C). Germline-specific ontologies were enriched only in EpiLC-specific KDM5C-bound
217 promoters, such as meiotic nuclear division (GO: 0007127 p.adjust = 6.77e-16) (Figure 5C). There were no
218 ontologies significantly enriched for PNC-specific KDM5C target genes. Using our mouse germline gene
219 list, we observed evident KDM5C signal around the TSS of many germline genes in EpiLCs, but not in
220 PNCs (Figure 5D). Based on our ChIP-seq peak cut-off criteria, KDM5C was highly enriched at 211 germline
221 gene promoters in EpiLCs (16.4% of all germline genes) (Figure 5E). Of note, KDM5C was only bound to
222 about one third of *Kdm5c*-KO RNA-seq DEG promoters (EpiLC only DEGs: 34.9%, Brain only DEGs: 30%)
223 (Supplementary figure 1A-C). However, KDM5C did bind the promoter of 4 out of the 5 genes dysregulated in
224 both the brain and EpiLCs (*D1Pas1*, *Hsf2bp*, *Cyct*, and *Stk31*). Representative examples of KDM5C-bound
225 and unbound EpiLC DEGs are *Dazl* and *Stra8*, respectively (Figure 5F). Together, these results demonstrate
226 KDM5C is recruited to a subset of germline genes in EpiLCs, including meiotic genes, but does not directly
227 regulate germline genes in neurons. Furthermore, the majority of germline mRNAs expressed in *Kdm5c*-KO
228 cells are dysregulated independent of direct KDM5C binding to their gene promoters.

229 Many germline-specific genes are suppressed by the polycomb repressive complex 1.6 (PRC1.6), which
230 contains transcription factor heterodimers E2F6/DP1 and MGA/MAX that respectively bind E2F and E-box
231 motifs⁵⁷. PRC1.6 members may recruit KDM5C to germline gene promoters¹³, given their association
232 with KDM5C in HeLa cells and ESCs^{45,58}. We thus used HOMER⁵⁹ to identify transcription factor motifs
233 enriched at KDM5C-bound or unbound germline gene promoters (TSS ± 500 bp, q-value < 0.1). MAX
234 and E2F6 binding sites were significantly enriched at germline genes bound by KDM5C in EpiLCs (MAX
235 q-value: 0.0068, E2F6 q-value: 0.0673, E2F q-value: 0.0917), but not at germline genes unbound by

236 KDM5C (Figure 5G). One third of KDM5C-bound promoters contained the consensus sequence for either
237 E2F6 (E2F, 5'-TCCCGC-3'), MGA (E-box, 5'-CACGTG-3'), or both, but only 17% of KDM5C-unbound genes
238 contained these motifs (Figure 5H). KDM5C-unbound germline genes were instead enriched for multiple
239 RFX transcription factor binding sites (RFX q-value < 0.0001, RFX2 q-value < 0.0001, RFX5 q-value <
240 0.0001) (Figure 5I, Supplementary figure 1D). RFX transcription factors bind X-box motifs⁶⁰ to promote
241 ciliogenesis^{61,62} and among them is RFX2, a central regulator of post-meiotic spermatogenesis^{63,64}. Although
242 *Rfx2* is also not a direct target of KDM5C (Supplementary figure 1E), RFX2 mRNA is derepressed in *Kdm5c-*
243 KO EpiLCs (Figure 5J). Thus, RFX2 is a candidate transcription factor for driving the ectopic expression of
244 many KDM5C-unbound germline genes in *Kdm5c*-KO cells.

245 **KDM5C is recruited to CpG islands at germline promoters to facilitate *de novo* DNA
246 methylation**

247 Previous work found two germline gene promoters have a marked reduction in DNA CpG methylation
248 (CpGme) in the *Kdm5c*-KO adult hippocampus¹³. Since histone 3 lysine 4 di- and trimethylation (H3K4me2/3)
249 impede *de novo* CpGme^{65,66}, KDM5C's removal of H3K4me2/3 may be required to suppress germline genes.
250 However, KDM5C's catalytic activity was recently shown to be dispensable for suppressing *Dazl* in ESCs⁴⁵. To
251 reconcile these observations, we hypothesized KDM5C erases H3K4me2/3 to promote the initial placement
252 of CpGme at germline gene promoters in EpiLCs.

253 To test this hypothesis, we first characterized KDM5C's expression as naïve ESCs differentiate into
254 EpiLCs (Figure 6A). While *Kdm5c* mRNA steadily decreased from 0 to 48 hours of differentiation (Figure
255 6B), KDM5C protein initially increased from 0 to 24 hours but then decreased to near knockout levels by 48
256 hours (Figure 6C). We then characterized KDM5C's substrates (H3K4me2/3) at germline gene promoters
257 with *Kdm5c* loss using published ChIP-seq datasets^{21,41}. *Kdm5c*-KO samples showed a marked increase in
258 H3K4me2 in EpiLCs (Figure 6D) and H3K4me3 in the amygdala (Figure 6E) around the TSS of germline
259 genes. Together, these data suggest KDM5C acts during the transition between ESCs and EpiLCs to remove
260 H3K4me2/3 at germline gene promoters.

261 Germline genes accumulate CpG methylation (CpGme) at CpG islands (CGIs) during the transition
262 from naïve to primed pluripotency^{18,20,67}. We first examined how many of our germline-enriched genes had
263 promoter CGIs (TSS ± 500 bp) using the UCSC genome browser⁶⁸. Notably, out of 1,288 germline-enriched
264 genes, only 356 (27.64%) had promoter CGIs (Figure 6F). CGI-containing germline genes had higher
265 enrichment of meiotic gene ontologies compared to CGI-free genes, including meiotic nuclear division
266 (GO:0140013, p.adjust = 2.17e-12) and meiosis I (GO:0007127, p.adjust = 3.91e-10) (Figure 6G). Germline
267 genes with promoter CGIs were more highly expressed than CGI-free genes across spermatogenesis
268 stages, with highest expression in meiotic spermatocytes (Figure 6H). Contrastingly, CGI-free genes only
269 displayed substantial expression in post-meiotic round spermatids (Figure 6H). Although only a minor portion

270 of germline gene promoters contained CGIs, CGIs strongly determined KDM5C's recruitment to germline
271 genes ($p = 2.37e-67$, Odds Ratio = 17.8, Fisher's exact test), with 79.15% of KDM5C-bound germline gene
272 promoters harboring CGIs (Figure 6G).

273 To assess how KDM5C loss impacts initial CpGme placement at germline gene promoters, we performed
274 whole genome bisulfite sequencing (WGBS) in male wild-type and *Kdm5c*-KO ESCs and 96-hour extend
275 EpiLCs (exEpiLCs), when germline genes reach peak methylation levels¹⁷ (Figure 6I). We first identified
276 which germline gene promoters significantly gained CpGme in wild-type cells during nESC to exEpiLCs
277 differentiation (methylKit⁶⁹, $q < 0.01$, $|methylation\ difference| > 25\%$, TSS \pm 500 bp). In wild-type cells, the
278 majority of germline genes gained substantial CpGme at their promoter during differentiation (60.08%),
279 regardless if their promoter contained a CGI (Figure 6J).

280 We then identified promoters differentially methylated in wild-type versus *Kdm5c*-KO exEpiLCs (methylKit,
281 $q < 0.01$, $|methylation\ difference| > 25\%$, TSS \pm 500 bp). Of the 48,882 promoters assessed, 274 promoters
282 were significantly hypomethylated and 377 promoters were significantly hypermethylated with KDM5C loss
283 (Supplementary figure 2A). Many promoters hyper- and hypomethylated in *Kdm5c*-KO exEpiLCs belonged to
284 genes with unknown functions. Hypomethylated promoters were significantly enriched for germline gene
285 ontologies, such as meiotic nuclear division (GO:0140013, $p.adjust = 0.012$) (Supplementary figure 2B),
286 with 10.22% of hypomethylated promoters belonging to germline genes. Approximately half of germline
287 promoters hypomethylated in *Kdm5c*-KO exEpiLCs are direct targets of KDM5C in EpiLCs (13 out of 28
288 hypomethylated promoters).

289 Promoters that showed the most robust loss of CpGme in *Kdm5c*-KO exEpiLCs (lowest q -values) harbored
290 CGIs (Figure 6K). CGI promoters, but not CGI-free promoters, had a significant reduction in CpGme with
291 KDM5C loss as a whole (Figure 6L) (Non-CGI promoters $p = 0.0846$, CGI promoters $p = 0.0081$, Mann-
292 Whitney U test). Significantly hypomethylated promoters included germline genes consistently dysregulated
293 across multiple *Kdm5c*-KO RNA-seq datasets¹³, such as *D1Pas1* (methylation difference = -60.03%, q -value
294 = 3.26e-153) and *Naa11* (methylation difference = -42.45%, q -value = 1.44e-38) (Figure 6M). Surprisingly,
295 we found only a modest reduction in CpGme at *Dazl*'s promoter (methylation difference = -6.525%, q -value
296 = 0.0159) (Figure 6N). Altogether, these results demonstrate KDM5C is recruited to germline gene CGIs
297 in EpiLCs to promote CpGme at germline gene promoters. Furthermore, this suggests while KDM5C's
298 catalytic activity is required for repression of some germline genes, some loci can compensate for KDM5C
299 loss through other silencing mechanisms, even when retaining H3K4me2/3 around the TSS.

300 Discussion

301 In the above study, we demonstrate KDM5C's pivotal role in the development of tissue identity. We first
302 characterized tissue-enriched genes expressed within the mouse *Kdm5c*-KO brain and identified substantial
303 derepression of testis, liver, muscle, and ovary-enriched genes. Testis genes significantly enriched within

304 the *Kdm5c*-KO amygdala and hippocampus are specific to the germline and not expressed within somatic
305 cells. *Kdm5c*-KO epiblast-like cells (EpiLCs) aberrantly express key drivers of germline identity and meiosis,
306 including *Dazl* and *Stra8*, while the adult brain primarily expresses genes important for late spermatogenesis.
307 We demonstrated that although *Kdm5c* mutant sex did not influence whether sperm or egg-specific genes
308 were misexpressed, female EpiLCs are more sensitive to germline gene de-repression. Germline genes
309 can become aberrantly expressed in *Kdm5c*-KO cells via an indirect mechanism, such as activation through
310 ectopic RFX transcription factors. Finally, we found KDM5C is dynamically regulated during ESC to EpiLC
311 differentiation to promote long-term germline gene silencing through DNA methylation at CpG islands.
312 Therefore, we propose KDM5C plays a fundamental role in the development of tissue identity during early
313 embryogenesis, including the establishment of the soma-germline boundary. By systematically characterizing
314 KDM5C's role in germline gene repression, we unveiled unique mechanisms governing the misexpression
315 distinct germline gene classes within somatic lineages. Furthermore, these data provide molecular footholds
316 which can be exploited to test the overarching contribution of ectopic germline gene expression upon
317 neurodevelopment.

318 By comparing *Kdm5c* mutant males and females, we revealed germline gene suppression is sexually
319 dimorphic. Although sex did not impact whether egg or sperm-specific genes were dysregulated, organismal
320 sex did greatly influence the degree of germline gene dysregulation. Female EpiLCs are more severely
321 impacted by loss of KDM5C-mediated germline gene suppression, yet this difference is not due to the
322 increased number of germline genes on the X chromosome^{52,53}. Increased female sensitivity to germline
323 gene de-repression may be related to females having a higher dose of KDM5C than males, due to its
324 escape from XCI^{48–51}. Intriguingly, females with heterozygous loss of *Kdm5c* also had over double the
325 number of germline DEGs than hemizygous knockout males, even though their level of KDM5C should
326 be roughly equivalent to that of wild-type males. Males could partially compensate for KDM5C's loss via
327 the Y-chromosome homolog, KDM5D, which exhibits weaker demethylase activity than KDM5C⁸. However,
328 KDM5D has not been reported to regulate germline gene expression. Altogether, these results suggests
329 germline gene silencing mechanisms differ between males and females, which warrants further study to
330 elucidate the biological ramifications and underlying mechanisms.

331 We found KDM5C is largely dispensable for promoting normal gene expression during development, yet is
332 critical for suppressing ectopic developmental programs. It is important to note that while we highlighted
333 KDM5C's regulation of germline genes, some germline-enriched genes like *Dazl* are also expressed at the
334 2-cell stage and in naïve ESCs/inner cell mass for their role in pluripotency and self-renewal^{40,45,70,71}. These
335 “self-renewal” germline genes are then silenced during ESC differentiation into epiblast stem cells/EpiLCs^{17,18}.
336 We found that while *Kdm5c*-KO EpiLCs express *Dazl*, they did not express 2-cell-specific genes like *Zscan4c*.
337 These data suggest the 2-cell-like state reported in *Kdm5c*-KO ESCs⁴⁵ likely reflects KDM5C's primary
338 role in germline gene repression. Germline gene misexpression in *Kdm5c*-KO EpiLCs may indicate they
339 are differentiating into primordial germ cell-like cells (PGCLCs)^{33,34,36}. Yet, *Kdm5c*-KO EpiLCs had normal

340 cellular morphology and properly expressed markers for primed pluripotency, including *Otx2* which blocks
341 EpiLC differentiation into PGCs/PGCLCs⁷². In addition to unimpaired EpiLC differentiation, *Kdm5c*-KO gross
342 brain morphology is overall normal¹² and hardly any brain-specific genes were significantly dysregulated.
343 Thus, ectopic germline gene expression occurs along with overall proper somatic differentiation in *Kdm5c*-KO
344 animals.

345 Our work provides novel insight into the cross-talk between H3K4me and CpGme, which are often
346 mutually exclusive⁷³. In EpiLCs, loss of KDM5C binding at a subset of germline gene promoters, e.g. *D1Pas1*
347 and *Naa11*, strongly impaired CGI methylation, and resulted in their long-lasting de-repression into adult-
348 hood. Removal of H3K4me2/3 at CGIs is a plausible mechanism for KDM5C-mediated germline gene
349 suppression^{13,54}, given H3K4me2/3 can oppose DNMT3 activity^{65,66}. However, emerging work indicates
350 many histone-modifying enzymes have non-catalytic functions that influence gene expression, sometimes
351 even more potently than their catalytic roles^{74,75}. Indeed, KDM5C's catalytic activity was recently found to be
352 dispensable for repressing *Dazl* in ESCs⁴⁵. In our study, *Dazl*'s promoter still gained CpGme in *Kdm5c*-KO
353 exEpiLCs, even with elevated H3K4me2. *Dazl* and a few other germline gene CGIs use multiple repressive
354 mechanisms to facilitate CpGme^{16,17,46,47}. This suggests alternative silencing mechanisms are sufficient to
355 recruit DNMT3s to some germline CGIs, while others may require KDM5C-mediated H3K4me removal to
356 overcome promoter CGI escape from CpGme^{73,76}. Furthermore, these results indicate the requirement for
357 catalytic activity can change depending upon the locus and developmental stage, even for the same class of
358 genes. Further experiments are required to determine if catalytically inactive KDM5C can suppress germline
359 genes at later developmental stages.

360 By generating a comprehensive list of mouse germline-enriched genes, we were able to reveal distinct
361 derepressive mechanisms governing early versus late-stage germline developmental programs. Previous
362 work on germline gene silencing has focused on genes with promoter CGIs^{18,73}, and indeed the major-
363 ity of KDM5C targets in EpiLCs were germ cell identity genes harboring CGIs. However, over 70% of
364 germline-enriched gene promoters lacked CGIs, including the many KDM5C-unbound germline genes
365 that were de-repressed in *Kdm5c*-KO cells. CGI-free, KDM5C-unbound germline genes were primarily
366 late-stage spermatogenesis genes and significantly enriched for RFX2 binding sites, a central regulator
367 of spermiogenesis^{63,64}. These data suggest that once activated during early embryogenesis, drivers of
368 germline identity like *Rfx2*, *Stra8*, and *Dazl* turn on downstream germline programs, ultimately culminating
369 in the expression of spermiogenesis genes in the adult *Kdm5c*-KO brain. Therefore, we propose KDM5C
370 is recruited via promoter CGIs to genes that shape germ cell formation to act as a break against runaway
371 activation of germline-specific programs.

372 The above work provides the mechanistic foundation for KDM5C-mediated repression of tissue and
373 germline-specific genes. However, the contribution of these ectopic, tissue-specific genes towards *Kdm5c*-
374 KO neurological impairments is still unknown. In addition to germline genes, we also identified significant
375 enrichment of muscle and liver-biased transcripts within the *Kdm5c*-KO brain. Intriguingly, select liver and

376 muscle-biased DEGs do have known roles within the brain, such as the liver-enriched lipid metabolism gene
377 *Apolipoprotein C-I* (*Apoc1*)²⁷. *APOC1* dysregulation is implicated in Alzheimer's disease in humans²⁸ and
378 overexpression of *Apoc1* in the mouse brain can impair learning and memory⁷⁷. KDM5C may therefore be
379 crucial for neurodevelopment by fine-tuning the expression of tissue-enriched, dosage-sensitive genes like
380 *Apoc1*.

381 Given germline genes have no known functions within the brain, their impact upon neurodevelopment
382 is currently unknown. In *C. elegans*, misexpression of germline genes due to loss of *Retinoblastoma*
383 (*Rb*) homologs results in enhanced piRNA signaling ectopic P granule formation in neurons^{78,79}. Ectopic
384 testicular germline transcripts have also been observed in a variety of cancers, including brain tumors in
385 *Drosophila* and mammals^{80,81} and shown to promote cancer progression^{82–84}. Intriguingly, mouse models and
386 human cells for other chromatin-linked neurodevelopmental disorders also display impaired soma-germline
387 demarcation^{7,85–88}, such as DNA methyltransferase 3b (DNMT3B), H3K9me1/2 methyltransferases G9A/GLP,
388 methyl-CpG -binding protein 2 (MECP2)⁸⁵. Recently, the transcription factor ZMYM2 (ZNF198), whose
389 mutation causes neurodevelopmental-craniofacial syndrome with variable renal and cardiac abnormalities
390 (OMIM #619522), was also shown to repress germline genes by promoting H3K4 methylation removal and
391 DNA methylation⁸⁹. Thus, KDM5C is among a growing cohort of neurodevelopmental disorders with similar
392 erosion of the germline versus soma boundary. Further research is required to determine the impact of these
393 germline genes and the extent to which this phenomenon occurs in humans.

394 Materials and Methods

395 Classifying tissue-enriched and germline-enriched genes

396 Tissue-enriched differentially expresssd genes (DEGs) were determined by their classification in a previ-
397 ously published dataset from 17 male and female mouse tissues²². This study defined tissue expression as
398 greater than 1 Fragments Per Kilobase of transcript per Million mapped read (FPKM) and tissue enrichment
399 as at least 4-fold higher expression than any other tissue.

400 We curated a list of germline-enriched genes using an RNA-seq dataset from wild-type and germline-
401 depleted (Kit^{W/W^v}) male and female mouse embryos from embryonic day 12, 14, and 16³², as well as adult
402 male testes²⁹. Germline-enriched genes met the following criteria: 1) their expression is greater than 1
403 FPKM in wild-type germline 2) their expression in any wild-type somatic tissues²² does not exceed 20%
404 of maximum expression in wild-type germline, and 3) their expression in the germ cell-depleted (Kit^{W/W^v})
405 germline, for any sex or time point, does not exceed 20% of maximum expression in wild-type germline. We
406 defined sperm and egg-biased genes as those whose expression in the opposite sex, at any time point, is no
407 greater than 20% of the gene's maximum expression in a given sex. Genes that did not meet this threshold
408 for either sex were classified as 'unbiased'.

409 **Cell culture**

410 We utilized our previously established cultures of male wild-type and *Kdm5c* knockout (-KO) embryonic
411 stem cells⁴¹. Sex was confirmed by genotyping *Uba1/Uba1y* on the X and Y chromosomes with the following
412 primers: 5'-TGGATGGTGTGCCAATG-3', 5'-CACCTGCACGTTGCCCT-3'. Deletion of *Kdm5c* was
413 confirmed through the primers 5'-ATGCCCATATTAAGAGTCCTG-3', 5'-TCTGCCTTGATGGGACTGTT-3',
414 and 5'-GGTTCTAACACTCACATAGTG-3'.

415 Embryonic stem cells (ESCs) and epiblast-like cells were cultured using previously established
416 methods³⁷. Briefly, ESCs were initially cultured in primed ESC (pESC) media consisting of KnockOut
417 DMEM (Gibco#10829-018), fetal bovine serum (Gibco#A5209501), KnockOut serum replacement
418 (Invitrogen#10828-028), Glutamax (Gibco#35050-061), Anti-Anti (Gibco#15240-062), MEM Non-essential
419 amino acids (Gibco#11140-050), and beta-mercaptoethanol (Sigma#M7522). They were then transitioned
420 into ground-state, "naïve" ESCs (nESCs) by culturing for four passages in N2B27 media containing
421 DMEM/F12 (Gibco#11330-032), Neurobasal media (Gibco#21103-049), Gluamax (Gibco#35050-061),
422 Anti-Anti (Gibco#15240-062), N2 supplement (Invitrogen#17502048), and B27 supplement without vitamin
423 A (Invitrogen#12587-010), and beta-mercaptoethanol. Both pESC and nESC media were supplemented
424 with 3 µM GSK3 inhibitor CHIR99021 (Sigma #SML1046-5MG), 1 µM MEK inhibitor PD0325901 (Sigma
425 #PZ0162-5MG), and 1,000 units/mL leukemia inhibitory factor (LIF, Millipore#ESG1107).

426 nESCs were differentiated into epiblast-like cells (EpiLCs, 48 hours) and extendend EpiLCs (exEpiLCs,
427 96 hours) by culturing in N2B27 media containing DMEM/F12, Neurobasal media, Gluamax, Anti-Anti,
428 N2 supplement, B27 supplement (Invitrogen#17504044), beta-mercaptoethanol, fibroblast growth factor 2
429 (FGF2, R&D Biotechne 233-FB), and activin A (R&D Biotechne 338AC050CF), as previously described³⁷.

430 **Real time quantitative PCR (RT-qPCR)**

431 nESCs were differentiated into EpiLCs as described above. Cells were lysed with Tri-reagent BD (Sigma
432 #T3809) at 0, 24, and 48 hours of differentiation. RNA was phase separated with 0.1 uL/uL 1-bromo-3-
433 chloropropane (Sigma #B9673) and then precipitated with isopropanol (Sigma #I9516). For each sample,
434 2 ug of RNA was reverse transcribed using the ProtoScript II Reverse transcriptase kit from New England
435 Biolabs (NEB #M0368S) and primed with oligo dT. Expression of *Kdm5c* was detected using the primers
436 5'-CCCATGGAGGCCAGAGAATAAG-3' 5'-CTCAGCGATAAGAGAATTGCTAC-3' and normalized to TBP
437 with the Power SYBR™ Green PCR Master Mix (ThermoFisher #4367659).

438 **Western Blot**

439 Total protein was extracted during nESC to EpiLC differentiation at 0, 24, and 48 hours by sonicating cells
440 at 20% amplitude for 15 seconds in 2X SDS sample buffer, then boiling at 100 °C for 10 minutes. Proteins
441 were separated on a 7.5% SDS page gel, transferred overnight onto a fluorescent membrane, blotted for

442 rabbit anti-KDM5C (in house, 1:500) and mouse anti-DAXX (Santa Cruz #(H-7): sc-8043, 1:500) imaged
443 using the LiCor Odyssey CLx system. Band intensity was quantified using ImageJ.

444 **RNA sequencing (RNA-seq) data analysis**

445 After ensuring read quality via FastQC (v0.11.8), reads were then mapped to the mm10 *Mus musculus*
446 genome (Gencode) using STAR (v2.5.3a), during which we removed duplicates and kept only uniquely
447 mapped reads. Count files were generated by FeatureCounts (Subread v1.5.0), and BAM files were
448 converted to bigwigs using deeptools (v3.1.3) and visualized by the UCSC genome browser. RStudio (v3.6.0)
449 was then used to analyze counts files by DESeq2 (v1.26.0)²³ to identify differentially expressed genes
450 (DEGs) with a q-value (p-adjusted via FDR/Benjamini–Hochberg correction) less than 0.1 and a log2 fold
451 change greater than 0.5. For all DESeq2 analyses, log2 fold changes were calculated with IfcShrink using
452 the ashR package⁹⁰. MA-plots were generated by ggpubr (v0.6.0), and Eulerr diagrams were generated by
453 eulerr (v6.1.1). Boxplots and scatterplots were generated by ggpubr (v0.6.0) and ggplot2 (v3.3.2). The Upset
454 plot was generated via the package UpSetR (v1.4.0)⁹¹. Gene ontology (GO) analyses were performed by
455 the R package enrichPlot (v1.16.2) using the biological processes setting and compareCluster.

456 **Chromatin immunoprecipitation followed by DNA sequencing (ChIP-seq) data analysis**

457 ChIP-seq reads were aligned to mm10 using Bowtie1 (v1.1.2) allowing up to two mismatches. Only
458 uniquely mapped reads were used for analysis. Peaks were called using MACS2 software (v2.2.9.1) using
459 input BAM files for normalization, with filters for a q-value < 0.1 and a fold enrichment > 1. We removed
460 “black-listed” genomic regions that often give aberrant signals. Common peak sets were obtained in R via
461 DiffBind[estrogen@ross-innesDifferentialOestrogenReceptor2012] (v3.6.5). In the case of KDM5C ChIP-seq,
462 *Kdm5c*-KO peaks were then subtracted from wild-type samples using bedtools (v2.25.0). Peak proximity
463 to genome annotations was determined by ChIPSeeker⁹² (v1.32.1). Gene ontology (GO) analyses were
464 performed by the R package enrichPlot (v1.16.2) using the biological processes setting and compareCluster.
465 Enriched motifs were identified using HOMER⁵⁹. Average binding across the genome was visualized using
466 deeptools (v3.1.3). Bigwigs were visualized using the UCSC genome browser.

467 **CpG island (CGI) analysis**

468 Locations of CpG islands were determined through the mm10 UCSC genome browser CpG island track⁶⁸,
469 which classified CGIs as regions that have greater than 50% GC content, are larger than 200 base pairs,
470 and have a ratio of CG dinucleotides observed over the expected amount greater than 0.6. CGI genomic
471 coordinates were then annotated using ChIPSeeker⁹² (v1.32.1) and filtered for ones that lie within promoters
472 of our germline-enriched genes (TSS ± 500).

473 **Whole genome bisulfite sequencing (WGBS)**

474 Genomic DNA (gDNA) from naïve ESCs and extended EpiLCs was extracted using the Wizard Genomic
475 DNA Purification Kit (Promega A1120), following the instructions for Tissue Culture Cells. gDNA from
476 two wild-types and two *Kdm5c*-KOs of each cell type was sent to Novogene for WGBS using the Illumina
477 NovaSeq X Plus platform and sequenced for 150bp paired-end reads (PE150). All samples had greater
478 than 99% bisulfite conversion rates. Reads were adapter and quality trimmed with Trim Galore (v0.6.10)
479 and aligned to the mm10 genome using Bismark⁹³ (v0.22.1). Analysis of differential methylation at germline
480 gene promoters was performed using methylKit⁶⁹ (v1.28.0) with a minimum coverage of 3 paired reads, a
481 percentage cut-off of 25%, and q-value of 0.01. methylKit was also used to calculate average percentage
482 methylation at germline gene promoters. Methylation bedgraph tracks were generated via Bismark and
483 visualized using the UCSC genome browser.

484 **Data availability**

485 **WGBS in wild-type and *Kdm5c*-KO ESCs and exEpiLCs**

486 XXXX

487 **Published datasets**

488 All published datasets are available at the Gene Expression Omnibus (GEO) <https://www.ncbi.nlm.nih>
489 .gov/geo. Published RNA-seq datasets analyzed in this study included the male wild-type and *Kdm5c*-KO
490 adult amygdala and hippocampus²¹ (available at GEO: GSE127722) and male wild-type and *Kdm5c*-KO
491 EpiLCs⁴¹ (available at GEO: GSE96797).

492 Previously published ChIP-seq experiments included KDM5C in wild-type and *Kdm5c*-KO EpiLCs⁴¹ (avail-
493 able at GEO: GSE96797) and mouse primary neuron cultures (PNCs) from the cortex and hippocampus¹²
494 (available at GEO: GSE61036). ChIP-seq of histone 3 lysine 4 dimethylation in male wild-type and *Kdm5c*-KO
495 EpiLCs⁴¹ is also available at GEO: GSE96797. ChIP-seq of histone 3 lysine 4 trimethylation in wild-type and
496 *Kdm5c*-KO male amygdala²¹ are available at GEO: GSE127817.

497 **Data analysis**

498 Scripts used to generate the results, tables, and figures of this study are available via the GitHub
499 repository: XXX

500 Acknowledgements

501 We thank Drs. Sundeep Kalantry, Milan Samanta, and Rebecca Malcore for providing protocols and
502 expertise in culturing mouse ESCs and EpiLCs, as well as providing wild-type and *Kdm5c*-KO ESCs used in
503 this study. We thank Dr. Jacob Mueller for his insight in germline gene regulation and directing us to the
504 germline-depleted mouse models. We also thank Drs. Kenneth Kwan, Natalie Tronson, Michael Sutton,
505 Stephanie Bielas, Donna Martin, and the members of the Iwase, Sutton, Bielas, and Martin labs for helpful
506 discussions and critiques of the data. We thank members of the University of Michigan Reproductive
507 Sciences Program for providing feedback throughout the development of this work. This work was supported
508 by grants from the National Institutes of Health (NIH) (National Institute of Neurological Disorders and Stroke:
509 NS089896, 5R21NS104774, and NS116008 to S.I.), Farrehi Family Foundation Grant (to S.I.), the University
510 of Michigan Career Training in Reproductive Biology (NIH T32HD079342, to K.M.B.), the NIH Early Stage
511 Training in the Neurosciences Training Grant (T32-NS076401 to K.M.B.), and the Michigan Predoctoral
512 Training in Genetics Grant (NIH T32GM007544, to I.V.)

513 Author contributions

514 K.M.B. and S.I. conceived the study and designed the experiments. I.V. generated the ESC and exEpiLC
515 WGBS data. K.M.B performed the data analysis and all other experiments. K.M.B and S.I. wrote and edited
516 the manuscript.

517 References

- 518 1. Strahl, B.D., and Allis, C.D. (2000). The language of covalent histone modifications. *Nature* **403**,
519 41–45. <https://doi.org/10.1038/47412>.
- 520 2. Jenuwein, T., and Allis, C.D. (2001). Translating the Histone Code. *Science* **293**, 1074–1080.
521 <https://doi.org/10.1126/science.1063127>.
- 522 3. Lewis, E.B. (1978). A gene complex controlling segmentation in *Drosophila*. *Nature* **276**, 565–570.
523 <https://doi.org/10.1038/276565a0>.
- 524 4. Kennison, J.A., and Tamkun, J.W. (1988). Dosage-dependent modifiers of polycomb and antennapedia
525 mutations in *Drosophila*. *Proc. Natl. Acad. Sci. U.S.A.* **85**, 8136–8140. <https://doi.org/10.1073/pnas.85.21.8136>.
- 526 5. Kassis, J.A., Kennison, J.A., and Tamkun, J.W. (2017). Polycomb and Trithorax Group Genes in
527 *Drosophila*. *Genetics* **206**, 1699–1725. <https://doi.org/10.1534/genetics.115.185116>.

- 528 6. Gabriele, M., Lopez Tobon, A., D'Agostino, G., and Testa, G. (2018). The chromatin basis of
529 neurodevelopmental disorders: Rethinking dysfunction along the molecular and temporal axes. *Prog
530 Neuropsychopharmacol Biol Psychiatry* *84*, 306–327. <https://doi.org/10.1016/j.pnpbp.2017.12.013>.
- 531 7. Schaefer, A., Sampath, S.C., Intrator, A., Min, A., Gertler, T.S., Surmeier, D.J., Tarakhovsky, A.,
532 and Greengard, P. (2009). Control of cognition and adaptive behavior by the GLP/G9a epigenetic
533 suppressor complex. *Neuron* *64*, 678–691. <https://doi.org/10.1016/j.neuron.2009.11.019>.
- 534 8. Iwase, S., Lan, F., Bayliss, P., De La Torre-Ubieta, L., Huarte, M., Qi, H.H., Whetstine, J.R., Bonni, A.,
535 Roberts, T.M., and Shi, Y. (2007). The X-Linked Mental Retardation Gene SMCX/JARID1C Defines a
Family of Histone H3 Lysine 4 Demethylases. *Cell* *128*, 1077–1088. <https://doi.org/10.1016/j.cell.2007.02.017>.
- 536 9. Claes, S., Devriendt, K., Van Goethem, G., Roelen, L., Meireleire, J., Raeymaekers, P., Cassiman,
537 J.J., and Fryns, J.P. (2000). Novel syndromic form of X-linked complicated spastic paraparesis. *Am J
Med Genet* *94*, 1–4.
- 538 10. Jensen, L.R., Amende, M., Gurok, U., Moser, B., Gimmel, V., Tschach, A., Janecke, A.R., Tariverdian,
539 G., Chelly, J., Fryns, J.P., et al. (2005). Mutations in the JARID1C gene, which is involved in
transcriptional regulation and chromatin remodeling, cause X-linked mental retardation. *Am J Hum
Genet* *76*, 227–236. <https://doi.org/10.1086/427563>.
- 540 11. Carmignac, V., Nambot, S., Lehalle, D., Callier, P., Moortgat, S., Benoit, V., Ghoumid, J., Delobel,
541 B., Smol, T., Thuillier, C., et al. (2020). Further delineation of the female phenotype with KDM5C
disease causing variants: 19 new individuals and review of the literature. *Clin Genet* *98*, 43–55.
<https://doi.org/10.1111/cge.13755>.
- 542 12. Iwase, S., Brookes, E., Agarwal, S., Badeaux, A.I., Ito, H., Vallianatos, C.N., Tomassy, G.S., Kasza, T.,
543 Lin, G., Thompson, A., et al. (2016). A Mouse Model of X-linked Intellectual Disability Associated with
Impaired Removal of Histone Methylation. *Cell Reports* *14*, 1000–1009. <https://doi.org/10.1016/j.celrep.2015.12.091>.
- 544 13. Scandaglia, M., Lopez-Atalaya, J.P., Medrano-Fernandez, A., Lopez-Cascales, M.T., Del Blanco, B.,
545 Lipinski, M., Benito, E., Olivares, R., Iwase, S., Shi, Y., et al. (2017). Loss of Kdm5c Causes Spurious
Transcription and Prevents the Fine-Tuning of Activity-Regulated Enhancers in Neurons. *Cell Rep* *21*,
47–59. <https://doi.org/10.1016/j.celrep.2017.09.014>.
- 546 14. Devlin, D.K., Ganley, A.R.D., and Takeuchi, N. (2023). A pan-metazoan view of germline-soma
547 distinction challenges our understanding of how the metazoan germline evolves. *Current Opinion in
Systems Biology* *36*, 100486. <https://doi.org/10.1016/j.coisb.2023.100486>.
- 547 15. Lehmann, R. (2012). Germline Stem Cells: Origin and Destiny. *Cell Stem Cell* *10*, 729–739.
<https://doi.org/10.1016/j.stem.2012.05.016>.

- 548 16. Endoh, M., Endo, T.A., Shinga, J., Hayashi, K., Farcas, A., Ma, K.W., Ito, S., Sharif, J., Endoh, T.,
Onaga, N., et al. (2017). PCGF6-PRC1 suppresses premature differentiation of mouse embryonic
549 stem cells by regulating germ cell-related genes. *eLife* 6. <https://doi.org/10.7554/eLife.21064>.
- 550 17. Mochizuki, K., Sharif, J., Shirane, K., Uranishi, K., Bogutz, A.B., Janssen, S.M., Suzuki, A., Okuda,
A., Koseki, H., and Lorincz, M.C. (2021). Repression of germline genes by PRC1.6 and SETDB1
in the early embryo precedes DNA methylation-mediated silencing. *Nat Commun* 12, 7020. <https://doi.org/10.1038/s41467-021-27345-x>.
- 551 18. Borgel, J., Guibert, S., Li, Y., Chiba, H., Schübeler, D., Sasaki, H., Forné, T., and Weber, M. (2010).
Targets and dynamics of promoter DNA methylation during early mouse development. *Nat Genet* 42,
553 1093–1100. <https://doi.org/10.1038/ng.708>.
- 554 19. Velasco, G., Hubé, F., Rollin, J., Neuillet, D., Philippe, C., Bouzinba-Segard, H., Galvani, A., Viegas-
Péquignot, E., and Francastel, C. (2010). Dnmt3b recruitment through E2F6 transcriptional repressor
mediates germ-line gene silencing in murine somatic tissues. *Proc Natl Acad Sci U S A* 107, 9281–
555 9286. <https://doi.org/10.1073/pnas.1000473107>.
- 556 20. Hackett, J.A., Reddington, J.P., Nestor, C.E., Dunican, D.S., Branco, M.R., Reichmann, J., Reik,
W., Surani, M.A., Adams, I.R., and Meehan, R.R. (2012). Promoter DNA methylation couples
genome-defence mechanisms to epigenetic reprogramming in the mouse germline. *Development*
557 139, 3623–3632. <https://doi.org/10.1242/dev.081661>.
- 558 21. Vallianatos, C.N., Raines, B., Porter, R.S., Bonefas, K.M., Wu, M.C., Garay, P.M., Collette, K.M.,
Seo, Y.A., Dou, Y., Keegan, C.E., et al. (2020). Mutually suppressive roles of KMT2A and KDM5C
in behaviour, neuronal structure, and histone H3K4 methylation. *Commun Biol* 3, 278. <https://doi.org/10.1038/s42003-020-1001-6>.
- 560 22. Li, B., Qing, T., Zhu, J., Wen, Z., Yu, Y., Fukumura, R., Zheng, Y., Gondo, Y., and Shi, L. (2017). A
Comprehensive Mouse Transcriptomic BodyMap across 17 Tissues by RNA-seq. *Sci Rep* 7, 4200.
561 <https://doi.org/10.1038/s41598-017-04520-z>.
- 562 23. Love, M.I., Huber, W., and Anders, S. (2014). Moderated estimation of fold change and dispersion for
563 RNA-seq data with DESeq2. *Genome Biol* 15, 550. <https://doi.org/10.1186/s13059-014-0550-8>.
- 564 24. Crackower, M.A., Kolas, N.K., Noguchi, J., Sarao, R., Kikuchi, K., Kaneko, H., Kobayashi, E., Kawai, Y.,
Kozieradzki, I., Landers, R., et al. (2003). Essential Role of Fkbp6 in Male Fertility and Homologous
565 Chromosome Pairing in Meiosis. *Science* 300, 1291–1295. <https://doi.org/10.1126/science.1083022>.
- 566 25. Xiol, J., Cora, E., Koglgruber, R., Chuma, S., Subramanian, S., Hosokawa, M., Reuter, M., Yang, Z.,
Berninger, P., Palencia, A., et al. (2012). A Role for Fkbp6 and the Chaperone Machinery in piRNA
Amplification and Transposon Silencing. *Molecular Cell* 47, 970–979. <https://doi.org/10.1016/j.molcel.2012.07.019>.

- 568 26. Cheng, S., Altmeppen, G., So, C., Welp, L.M., Penir, S., Ruhwedel, T., Menelaou, K., Harasimov, K.,
569 Stützer, A., Blayney, M., et al. (2022). Mammalian oocytes store mRNAs in a mitochondria-associated
membraneless compartment. *Science* *378*, eabq4835. <https://doi.org/10.1126/science.abq4835>.
- 570 27. Rouland, A., Masson, D., Lagrost, L., Vergès, B., Gautier, T., and Bouillet, B. (2022). Role of
571 apolipoprotein C1 in lipoprotein metabolism, atherosclerosis and diabetes: A systematic review.
Cardiovasc Diabetol *21*, 272. <https://doi.org/10.1186/s12933-022-01703-5>.
- 572 28. Leduc, V., Jasmin-Bélanger, S., and Poirier, J. (2010). APOE and cholesterol homeostasis in
573 Alzheimer's disease. *Trends in Molecular Medicine* *16*, 469–477. <https://doi.org/10.1016/j.molmed.2010.07.008>.
- 574 29. Mueller, J.L., Skaletsky, H., Brown, L.G., Zaghlul, S., Rock, S., Graves, T., Auger, K., Warren,
575 W.C., Wilson, R.K., and Page, D.C. (2013). Independent specialization of the human and mouse X
chromosomes for the male germ line. *Nat Genet* *45*, 1083–1087. <https://doi.org/10.1038/ng.2705>.
- 576 30. Handel, M.A., and Eppig, J.J. (1979). Sertoli Cell Differentiation in the Testes of Mice Genetically
577 Deficient in Germ Cells. *Biology of Reproduction* *20*, 1031–1038. <https://doi.org/10.1095/biolreprod20.5.1031>.
- 578 31. Green, C.D., Ma, Q., Manske, G.L., Shami, A.N., Zheng, X., Marini, S., Moritz, L., Sultan, C.,
579 Gurczynski, S.J., Moore, B.B., et al. (2018). A Comprehensive Roadmap of Murine Spermatogenesis
Defined by Single-Cell RNA-Seq. *Dev Cell* *46*, 651–667.e10. <https://doi.org/10.1016/j.devcel.2018.07.025>.
- 580 32. Soh, Y.Q., Junker, J.P., Gill, M.E., Mueller, J.L., van Oudenaarden, A., and Page, D.C. (2015). A
581 Gene Regulatory Program for Meiotic Prophase in the Fetal Ovary. *PLoS Genet* *11*, e1005531.
<https://doi.org/10.1371/journal.pgen.1005531>.
- 582 33. Magnúsdóttir, E., and Surani, M.A. (2014). How to make a primordial germ cell. *Development* *141*,
583 245–252. <https://doi.org/10.1242/dev.098269>.
- 584 34. Günesdogan, U., Magnúsdóttir, E., and Surani, M.A. (2014). Primordial germ cell specification: A
585 context-dependent cellular differentiation event [corrected]. *Philos Trans R Soc Lond B Biol Sci* *369*.
<https://doi.org/10.1098/rstb.2013.0543>.
- 586 35. Bardot, E.S., and Hadjantonakis, A.-K. (2020). Mouse gastrulation: Coordination of tissue patterning,
specification and diversification of cell fate. *Mechanisms of Development* *163*, 103617. <https://doi.org/10.1016/j.mod.2020.103617>.
- 588 36. Hayashi, K., Ohta, H., Kurimoto, K., Aramaki, S., and Saitou, M. (2011). Reconstitution of the
589 mouse germ cell specification pathway in culture by pluripotent stem cells. *Cell* *146*, 519–532.
<https://doi.org/10.1016/j.cell.2011.06.052>.
- 590 37. Samanta, M., and Kalantry, S. (2020). Generating primed pluripotent epiblast stem cells: A methodol-
ogy chapter. *Curr Top Dev Biol* *138*, 139–174. <https://doi.org/10.1016/bs.ctdb.2020.01.005>.

- 591
- 592 38. Welling, M., Chen, H., Muñoz, J., Musheev, M.U., Kester, L., Junker, J.P., Mischerikow, N., Arbab, M.,
Kuijk, E., Silberstein, L., et al. (2015). DAZL regulates Tet1 translation in murine embryonic stem cells.
EMBO Reports 16, 791–802. <https://doi.org/10.15252/embr.201540538>.
- 593
- 594 39. Macfarlan, T.S., Gifford, W.D., Driscoll, S., Lettieri, K., Rowe, H.M., Bonanomi, D., Firth, A., Singer, O.,
Trono, D., and Pfaff, S.L. (2012). Embryonic stem cell potency fluctuates with endogenous retrovirus
activity. Nature 487, 57–63. <https://doi.org/10.1038/nature11244>.
- 595
- 596 40. Suzuki, A., Hirasaki, M., Hishida, T., Wu, J., Okamura, D., Ueda, A., Nishimoto, M., Nakachi, Y.,
Mizuno, Y., Okazaki, Y., et al. (2016). Loss of MAX results in meiotic entry in mouse embryonic and
597 germline stem cells. Nat Commun 7, 11056. <https://doi.org/10.1038/ncomms11056>.
- 598 41. Samanta, M.K., Gayen, S., Harris, C., Maclary, E., Murata-Nakamura, Y., Malcore, R.M., Porter, R.S.,
Garay, P.M., Vallianatos, C.N., Samollow, P.B., et al. (2022). Activation of Xist by an evolutionarily
conserved function of KDM5C demethylase. Nat Commun 13, 2602. <https://doi.org/10.1038/s41467-022-30352-1>.
- 599
- 600 42. Koubova, J., Menke, D.B., Zhou, Q., Capel, B., Griswold, M.D., and Page, D.C. (2006). Retinoic
acid regulates sex-specific timing of meiotic initiation in mice. Proc. Natl. Acad. Sci. U.S.A. 103,
601 2474–2479. <https://doi.org/10.1073/pnas.0510813103>.
- 602 43. Lin, Y., Gill, M.E., Koubova, J., and Page, D.C. (2008). Germ Cell-Intrinsic and -Extrinsic Factors
Govern Meiotic Initiation in Mouse Embryos. Science 322, 1685–1687. <https://doi.org/10.1126/science.1166340>.
- 603
- 604 44. Endo, T., Mikedis, M.M., Nicholls, P.K., Page, D.C., and De Rooij, D.G. (2019). Retinoic Acid and Germ
605 Cell Development in the Ovary and Testis. Biomolecules 9, 775. <https://doi.org/10.3390/biom9120775>.
- 606 45. Gupta, N., Yakhou, L., Albert, J.R., Azogui, A., Ferry, L., Kirsh, O., Miura, F., Battault, S., Yamaguchi,
K., Laisné, M., et al. (2023). A genome-wide screen reveals new regulators of the 2-cell-like cell state.
607 Nat Struct Mol Biol. <https://doi.org/10.1038/s41594-023-01038-z>.
- 608 46. Pohlers, M., Truss, M., Frede, U., Scholz, A., Strehle, M., Kuban, R.-J., Hoffmann, B., Morkel, M.,
Birchmeier, C., and Hagemeier, C. (2005). A Role for E2F6 in the Restriction of Male-Germ-Cell-
609 Specific Gene Expression. Current Biology 15, 1051–1057. <https://doi.org/10.1016/j.cub.2005.04.060>.
- 610 47. Dahlet, T., Truss, M., Frede, U., Al Adhami, H., Bardet, A.F., Dumas, M., Vallet, J., Chicher, J.,
Hammann, P., Kottnik, S., et al. (2021). E2F6 initiates stable epigenetic silencing of germline genes
611 during embryonic development. Nat Commun 12, 3582. <https://doi.org/10.1038/s41467-021-23596-w>.
- 612 48. Agulnik, A.I., Mitchell, M.J., Mattei, M.G., Borsani, G., Avner, P.A., Lerner, J.L., and Bishop, C.E.
(1994). A novel X gene with a widely transcribed Y-linked homologue escapes X-inactivation in mouse
613 and human. Hum Mol Genet 3, 879–884. <https://doi.org/10.1093/hmg/3.6.879>.

- 614 49. Carrel, L., Hunt, P.A., and Willard, H.F. (1996). Tissue and lineage-specific variation in inactive
615 X chromosome expression of the murine Smcx gene. *Hum Mol Genet* 5, 1361–1366. <https://doi.org/10.1093/hmg/5.9.1361>.
- 616 50. Sheardown, S., Norris, D., Fisher, A., and Brockdorff, N. (1996). The mouse Smcx gene exhibits
617 developmental and tissue specific variation in degree of escape from X inactivation. *Hum Mol Genet*
618 5, 1355–1360. <https://doi.org/10.1093/hmg/5.9.1355>.
- 619 51. Xu, J., Deng, X., and Disteche, C.M. (2008). Sex-Specific Expression of the X-Linked Histone
Demethylase Gene Jarid1c in Brain. *PLoS ONE* 3, e2553. <https://doi.org/10.1371/journal.pone.0002553>.
- 620 52. Wang, P.J., McCarrey, J.R., Yang, F., and Page, D.C. (2001). An abundance of X-linked genes
621 expressed in spermatogonia. *Nat Genet* 27, 422–426. <https://doi.org/10.1038/86927>.
- 622 53. Khil, P.P., Smirnova, N.A., Romanienko, P.J., and Camerini-Otero, R.D. (2004). The mouse X
chromosome is enriched for sex-biased genes not subject to selection by meiotic sex chromosome
623 inactivation. *Nat Genet* 36, 642–646. <https://doi.org/10.1038/ng1368>.
- 624 54. Al Adhami, H., Vallet, J., Schaal, C., Schumacher, P., Bardet, A.F., Dumas, M., Chicher, J., Hammann,
P., Daujat, S., and Weber, M. (2023). Systematic identification of factors involved in the silencing
of germline genes in mouse embryonic stem cells. *Nucleic Acids Research* 51, 3130–3149. <https://doi.org/10.1093/nar/gkad071>.
- 625 55. Hurlin, P.J. (1999). Mga, a dual-specificity transcription factor that interacts with Max and contains a
T-domain DNA-binding motif. *The EMBO Journal* 18, 7019–7028. <https://doi.org/10.1093/emboj/18.2.4.7019>.
- 626 56. Tatsumi, D., Hayashi, Y., Endo, M., Kobayashi, H., Yoshioka, T., Kiso, K., Kanno, S., Nakai, Y., Maeda,
I., Mochizuki, K., et al. (2018). DNMTs and SETDB1 function as co-repressors in MAX-mediated
repression of germ cell-related genes in mouse embryonic stem cells. *PLoS ONE* 13, e0205969.
627 <https://doi.org/10.1371/journal.pone.0205969>.
- 628 57. Stielow, B., Finkernagel, F., Stiewe, T., Nist, A., and Suske, G. (2018). MGA, L3MBTL2 and E2F6
determine genomic binding of the non-canonical Polycomb repressive complex PRC1.6. *PLoS Genet*
629 14, e1007193. <https://doi.org/10.1371/journal.pgen.1007193>.
- 630 58. Tahiliani, M., Mei, P., Fang, R., Leonor, T., Rutenberg, M., Shimizu, F., Li, J., Rao, A., and Shi, Y.
(2007). The histone H3K4 demethylase SMCX links REST target genes to X-linked mental retardation.
631 *Nature* 447, 601–605. <https://doi.org/10.1038/nature05823>.
- 632 59. Heinz, S., Benner, C., Spann, N., Bertolino, E., Lin, Y.C., Laslo, P., Cheng, J.X., Murre, C., Singh, H.,
and Glass, C.K. (2010). Simple Combinations of Lineage-Determining Transcription Factors Prime
cis-Regulatory Elements Required for Macrophage and B Cell Identities. *Molecular Cell* 38, 576–589.
633 <https://doi.org/10.1016/j.molcel.2010.05.004>.

- 635
- 636 60. Gajiwala, K.S., Chen, H., Cornille, F., Roques, B.P., Reith, W., Mach, B., and Burley, S.K. (2000).
637 Structure of the winged-helix protein hRFX1 reveals a new mode of DNA binding. *Nature* **403**,
916–921. <https://doi.org/10.1038/35002634>.
- 638 61. Swoboda, P., Adler, H.T., and Thomas, J.H. (2000). The RFX-Type Transcription Factor DAF-19
639 Regulates Sensory Neuron Cilium Formation in *C. elegans*. *Molecular Cell* **5**, 411–421. [https://doi.org/10.1016/S1097-2765\(00\)80436-0](https://doi.org/10.1016/S1097-2765(00)80436-0).
- 640 62. Ashique, A.M., Choe, Y., Karlen, M., May, S.R., Phamluong, K., Solloway, M.J., Ericson, J., and
641 Peterson, A.S. (2009). The Rfx4 Transcription Factor Modulates Shh Signaling by Regional Control of
Ciliogenesis. *Sci. Signal.* **2**. <https://doi.org/10.1126/scisignal.2000602>.
- 642 63. Kistler, W.S., Baas, D., Lemeille, S., Paschaki, M., Seguin-Estevez, Q., Barras, E., Ma, W., Duteyrat, J.-
L., Morlé, L., Durand, B., et al. (2015). RFX2 Is a Major Transcriptional Regulator of Spermiogenesis.
643 *PLoS Genet* **11**, e1005368. <https://doi.org/10.1371/journal.pgen.1005368>.
- 644 64. Wu, Y., Hu, X., Li, Z., Wang, M., Li, S., Wang, X., Lin, X., Liao, S., Zhang, Z., Feng, X., et al.
645 (2016). Transcription Factor RFX2 Is a Key Regulator of Mouse Spermiogenesis. *Sci Rep* **6**, 20435.
<https://doi.org/10.1038/srep20435>.
- 646 65. Otani, J., Nankumo, T., Arita, K., Inamoto, S., Ariyoshi, M., and Shirakawa, M. (2009). Structural basis
647 for recognition of H3K4 methylation status by the DNA methyltransferase 3A ATRX–DNMT3–DNMT3L
domain. *EMBO Reports* **10**, 1235–1241. <https://doi.org/10.1038/embor.2009.218>.
- 648 66. Guo, X., Wang, L., Li, J., Ding, Z., Xiao, J., Yin, X., He, S., Shi, P., Dong, L., Li, G., et al. (2015).
649 Structural insight into autoinhibition and histone H3-induced activation of DNMT3A. *Nature* **517**,
640–644. <https://doi.org/10.1038/nature13899>.
- 650 67. Meissner, A., Mikkelsen, T.S., Gu, H., Wernig, M., Hanna, J., Sivachenko, A., Zhang, X., Bernstein,
B.E., Nusbaum, C., Jaffe, D.B., et al. (2008). Genome-scale DNA methylation maps of pluripotent and
651 differentiated cells. *Nature* **454**, 766–770. <https://doi.org/10.1038/nature07107>.
- 652 68. Nassar, L.R., Barber, G.P., Benet-Pagès, A., Casper, J., Clawson, H., Diekhans, M., Fischer, C.,
Gonzalez, J.N., Hinrichs, A.S., Lee, B.T., et al. (2023). The UCSC Genome Browser database: 2023
653 update. *Nucleic Acids Research* **51**, D1188–D1195. <https://doi.org/10.1093/nar/gkac1072>.
- 654 69. Akalin, A., Kormaksson, M., Li, S., Garrett-Bakelman, F.E., Figueiroa, M.E., Melnick, A., and Mason,
C.E. (2012). methylKit: A comprehensive R package for the analysis of genome-wide DNA methylation
655 profiles. *Genome Biol* **13**, R87. <https://doi.org/10.1186/gb-2012-13-10-r87>.
- 656 70. Torres-Padilla, M.-E. (2020). On transposons and totipotency. *Philos Trans R Soc Lond B Biol Sci*
657 **375**, 20190339. <https://doi.org/10.1098/rstb.2019.0339>.

- 658 71. Yang, M., Yu, H., Yu, X., Liang, S., Hu, Y., Luo, Y., Izsvák, Z., Sun, C., and Wang, J. (2022). Chemical-induced chromatin remodeling reprograms mouse ESCs to totipotent-like stem cells. *Cell Stem Cell* 29, 400–418.e13. <https://doi.org/10.1016/j.stem.2022.01.010>.
- 659
- 660 72. Zhang, J., Zhang, M., Acampora, D., Vojtek, M., Yuan, D., Simeone, A., and Chambers, I. (2018). OTX2 restricts entry to the mouse germline. *Nature* 562, 595–599. <https://doi.org/10.1038/s41586-018-0581-5>.
- 661
- 662 73. Weber, M., Hellmann, I., Stadler, M.B., Ramos, L., Pääbo, S., Rebhan, M., and Schübeler, D. (2007). Distribution, silencing potential and evolutionary impact of promoter DNA methylation in the human genome. *Nat Genet* 39, 457–466. <https://doi.org/10.1038/ng1990>.
- 663
- 664 74. Aubert, Y., Egolf, S., and Capell, B.C. (2019). The Unexpected Noncatalytic Roles of Histone Modifiers in Development and Disease. *Trends in Genetics* 35, 645–657. <https://doi.org/10.1016/j.tig.2019.06.004>.
- 665
- 666 75. Morgan, M.A.J., and Shilatifard, A. (2020). Reevaluating the roles of histone-modifying enzymes and their associated chromatin modifications in transcriptional regulation. *Nat Genet* 52, 1271–1281. <https://doi.org/10.1038/s41588-020-00736-4>.
- 667
- 668 76. Long, H.K., King, H.W., Patient, R.K., Odom, D.T., and Klose, R.J. (2016). Protection of CpG islands from DNA methylation is DNA-encoded and evolutionarily conserved. *Nucleic Acids Res* 44, 6693–6706. <https://doi.org/10.1093/nar/gkw258>.
- 669
- 670 77. Abildayeva, K., Berbée, J.F.P., Blokland, A., Jansen, P.J., Hoek, F.J., Meijer, O., Lütjohann, D., Gautier, T., Pillot, T., De Vente, J., et al. (2008). Human apolipoprotein C-I expression in mice impairs learning and memory functions. *Journal of Lipid Research* 49, 856–869. <https://doi.org/10.1194/jlr.M700518JLR200>.
- 671
- 672 78. Wang, D., Kennedy, S., Conte, D., Kim, J.K., Gabel, H.W., Kamath, R.S., Mello, C.C., and Ruvkun, G. (2005). Somatic misexpression of germline P granules and enhanced RNA interference in retinoblastoma pathway mutants. *Nature* 436, 593–597. <https://doi.org/10.1038/nature04010>.
- 673
- 674 79. Wu, X., Shi, Z., Cui, M., Han, M., and Ruvkun, G. (2012). Repression of germline RNAi pathways in somatic cells by retinoblastoma pathway chromatin complexes. *PLoS Genet* 8, e1002542. <https://doi.org/10.1371/journal.pgen.1002542>.
- 675
- 676 80. Nielsen, A.Y., and Gjerstorff, M.F. (2016). Ectopic Expression of Testis Germ Cell Proteins in Cancer and Its Potential Role in Genomic Instability. *Int J Mol Sci* 17. <https://doi.org/10.3390/ijms17060890>.
- 677
- 678 81. Adebayo Babatunde, K., Najafi, A., Salehipour, P., Modarressi, M.H., and Mobasher, M.B. (2017). Cancer/Testis genes in relation to sperm biology and function. *Iranian Journal of Basic Medical Sciences* 20. <https://doi.org/10.22038/ijbms.2017.9259>.
- 679

- 680 82. Janic, A., Mendizabal, L., Llamazares, S., Rossell, D., and Gonzalez, C. (2010). Ectopic expression
681 of germline genes drives malignant brain tumor growth in *Drosophila*. *Science* *330*, 1824–1827.
<https://doi.org/10.1126/science.1195481>.
- 682 83. Ghafouri-Fard, S., and Modarressi, M.-H. (2012). Expression of Cancer–Testis Genes in Brain Tumors:
683 Implications for Cancer Immunotherapy. *Immunotherapy* *4*, 59–75. <https://doi.org/10.2217/imt.11.145>.
- 684 84. Nin, D.S., and Deng, L.-W. (2023). Biology of Cancer-Testis Antigens and Their Therapeutic Implica-
685 tions in Cancer. *Cells* *12*, 926. <https://doi.org/10.3390/cells12060926>.
- 686 85. Bonefas, K.M., and Iwase, S. (2021). Soma-to-germline transformation in chromatin-linked neurode-
687 velopmental disorders? *FEBS J.* <https://doi.org/10.1111/febs.16196>.
- 688 86. Velasco, G., Walton, E.L., Sterlin, D., Héduin, S., Nitta, H., Ito, Y., Fouyssac, F., Mégarbané, A.,
689 Sasaki, H., Picard, C., et al. (2014). Germline genes hypomethylation and expression define a
molecular signature in peripheral blood of ICF patients: Implications for diagnosis and etiology.
Orphanet J Rare Dis *9*, 56. <https://doi.org/10.1186/1750-1172-9-56>.
- 690 87. Walton, E.L., Francastel, C., and Velasco, G. (2014). Dnmt3b Prefers Germ Line Genes and Cen-
691 tromeric Regions: Lessons from the ICF Syndrome and Cancer and Implications for Diseases. *Biology*
(Basel) *3*, 578–605. <https://doi.org/10.3390/biology3030578>.
- 692 88. Samaco, R.C., Mandel-Brehm, C., McGraw, C.M., Shaw, C.A., McGill, B.E., and Zoghbi, H.Y. (2012).
Crh and Oprm1 mediate anxiety-related behavior and social approach in a mouse model of MECP2
693 duplication syndrome. *Nat Genet* *44*, 206–211. <https://doi.org/10.1038/ng.1066>.
- 694 89. Graham-Paquin, A.-L., Saini, D., Sirois, J., Hossain, I., Katz, M.S., Zhuang, Q.K.-W., Kwon, S.Y.,
Yamanaka, Y., Bourque, G., Bouchard, M., et al. (2023). ZMYM2 is essential for methylation of
695 germline genes and active transposons in embryonic development. *Nucleic Acids Research*, gkad540.
<https://doi.org/10.1093/nar/gkad540>.
- 696 90. Stephens, M. (2016). False discovery rates: A new deal. *Biostat*, kxw041. <https://doi.org/10.1093/biostatistics/kxw041>.
- 698 91. Conway, J.R., Lex, A., and Gehlenborg, N. (2017). UpSetR: An R package for the visualization of
699 intersecting sets and their properties. *Bioinformatics* *33*, 2938–2940. <https://doi.org/10.1093/bioinformatics/btx364>.
- 700 92. Yu, G., Wang, L.G., and He, Q.Y. (2015). ChIPseeker: An R/Bioconductor package for ChIP peak
701 annotation, comparison and visualization. *Bioinformatics* *31*, 2382–2383. <https://doi.org/10.1093/bioinformatics/btv145>.
- 702 93. Krueger, F., and Andrews, S.R. (2011). Bismark: A flexible aligner and methylation caller for Bisulfite-
703 Seq applications. *Bioinformatics* *27*, 1571–1572. <https://doi.org/10.1093/bioinformatics/btr167>.

704 **Figures and Tables**

- 705 • Supplementary table 1: list of all germline genes.
- 706 – Columns to include:
- 707 * KDM5C bound vs not
- 708 * Log2fc in EpiLC, brain (separate columns?)
- 709 – CGI vs non

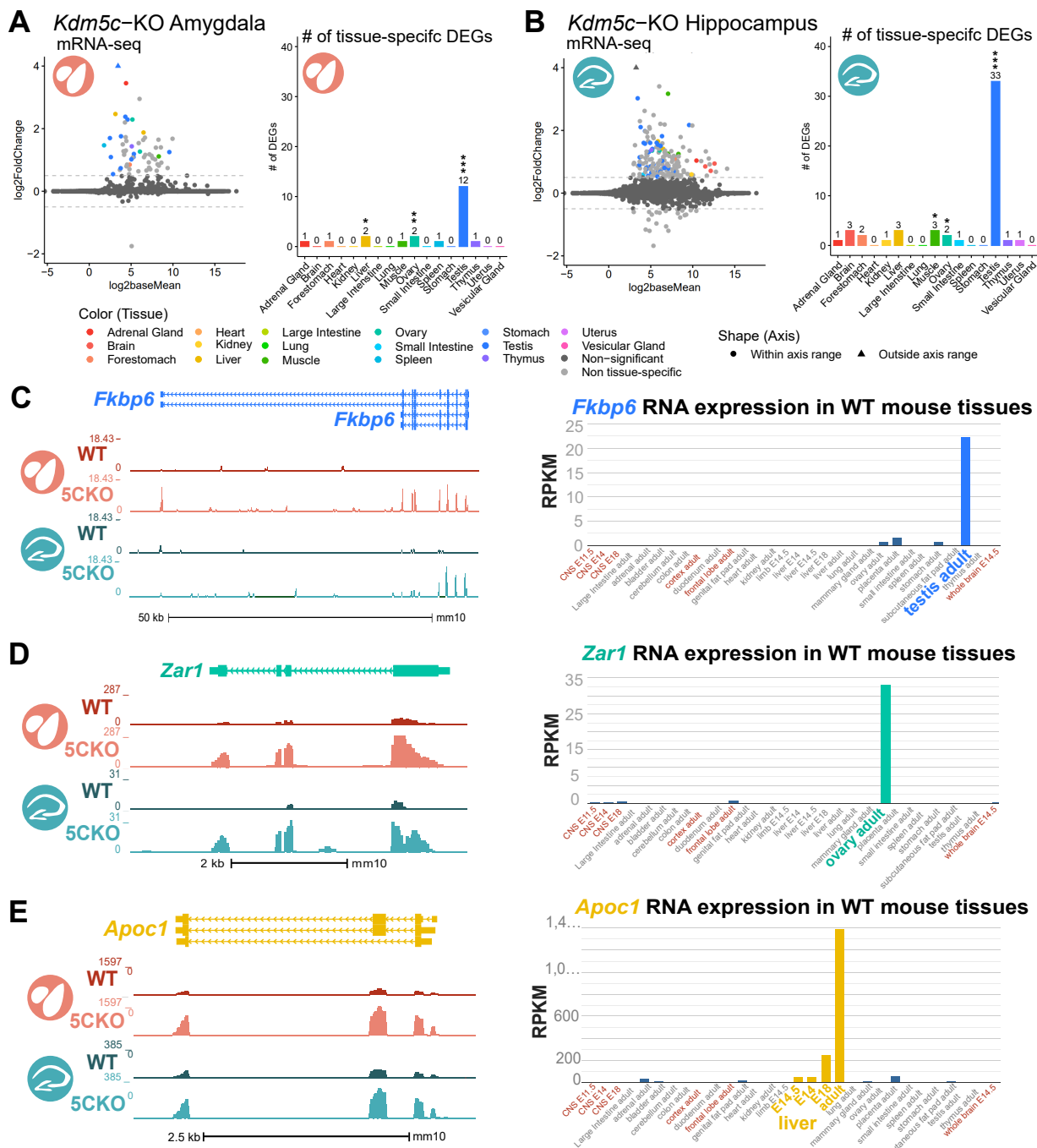


Figure 1: Tissue-enriched genes are misexpressed in the *Kdm5c*-KO brain. **A-B.** Expression of tissue-enriched genes (Li et al 2017) in the male *Kdm5c*-KO amygdala (A) and hippocampus (B). Left - MA plot of mRNA-sequencing. Right - Number of tissue-enriched differentially expressed genes (DEGs). * $p < 0.05$, ** $p < 0.01$, *** $p < 0.001$, Fisher's exact test. **C.** Left - UCSC browser view of an example aberrantly expressed testis-enriched DEG, *FK506 binding protein 6* (*Fkbp6*) in the wild-type (WT) and *Kdm5c*-KO (5CKO) amygdala (red) and hippocampus (teal) (Average, $n = 4$). Right - Expression of *Cyct* in wild-type tissues from NCBI Gene, with testis highlighted in blue and brain tissues highlighted in red. **D.** Left - UCSC browser view of an example ovary-enriched DEG, *Zygotic arrest 1* (*Zar1*). Right - Expression of *Zar1* in wild-type tissues from NCBI Gene, with ovary highlighted in teal and brain tissues highlighted in red. **E.** Left - UCSC browser view of an example liver-enriched DEG, *Apolipoprotein C-I* (*Apoc1*). Right - Expression of *Apoc1* in wild-type tissues from NCBI Gene, with liver highlighted in orange and brain tissues highlighted in red.

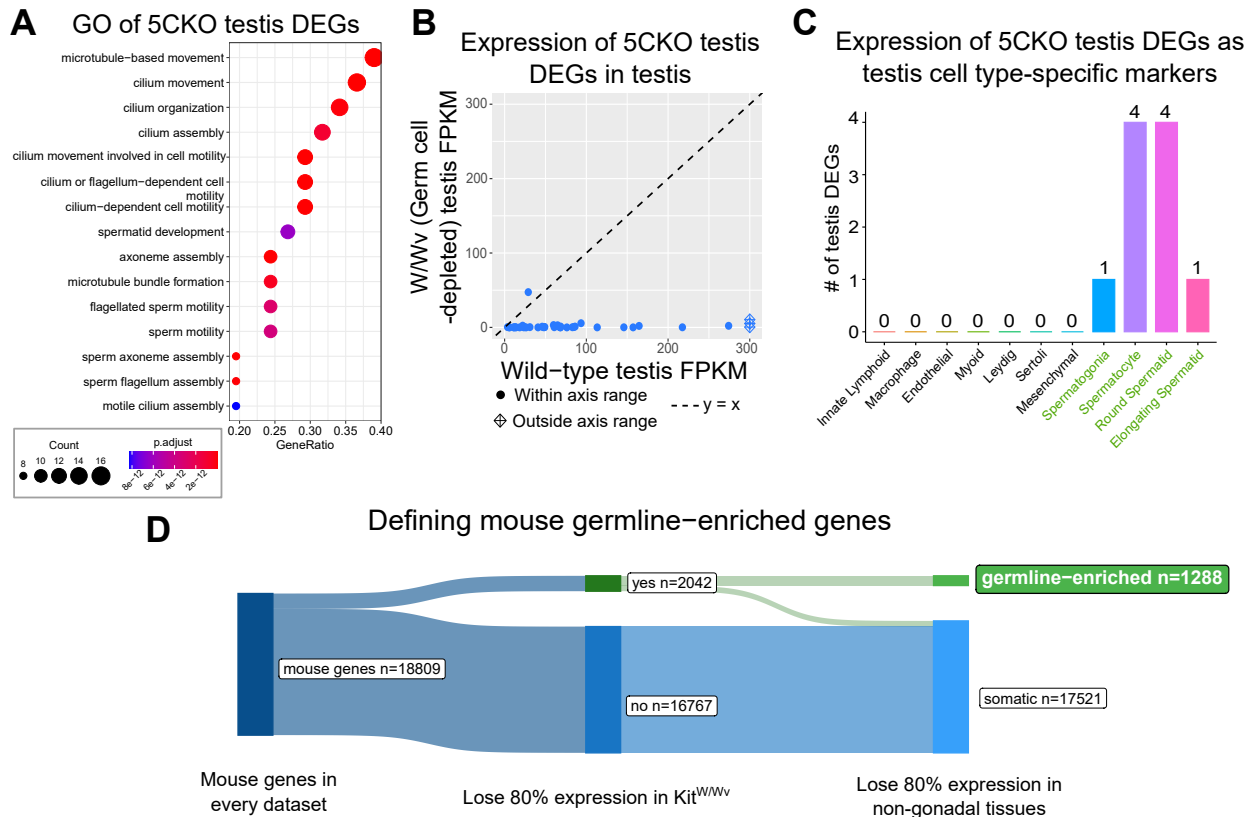


Figure 2: Aberrant transcription of germline genes in the *Kdm5c*-KO in the brain. **A.** enrichPlot gene ontology (GO) of *Kdm5c*-KO amygdala and hippocampus testis-enriched DEGs **B.** Expression of testis DEGs in wild-type (WT) testis versus germ cell-depleted (W/Wv) testis (Mueller et al 2013). Expression is in Fragments Per Kilobase of transcript per Million mapped reads (FPKM). **C.** Number of testis DEGs that were classified as cell-type specific markers in a single cell RNA-seq dataset of the testis (Green et al 2018). Germline cell types are highlighted in green, somatic cell types in black. **D.** Sankey diagram of mouse genes filtered for germline enrichment based on their expression in wild-type and W/Wv mice and in adult mouse non-gonadal tissues (Li et al 2017).

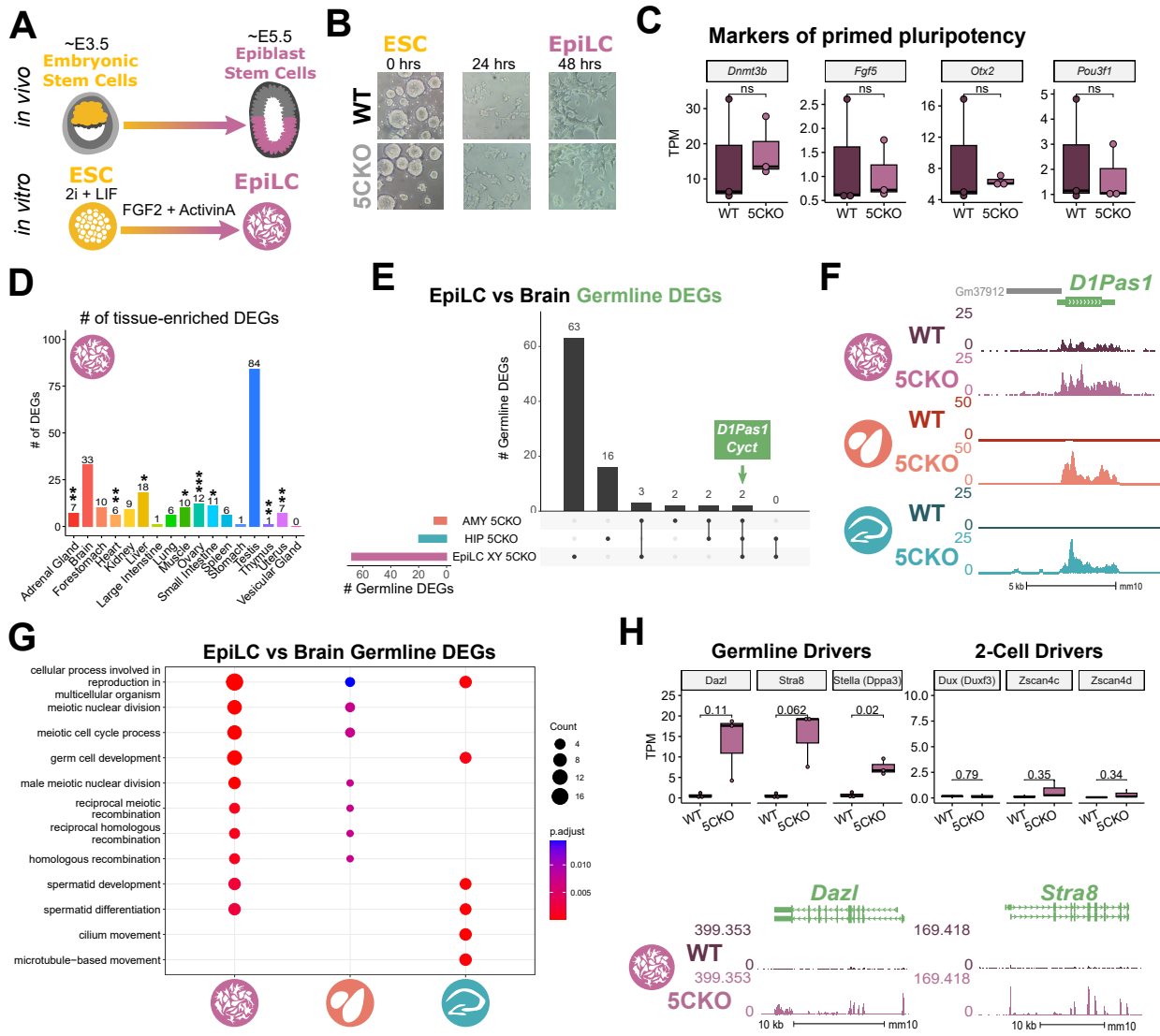


Figure 3: Kdm5c-KO epiblast-like cells express key drivers of germline identity **A.** Top - Diagram of *in vivo* differentiation of embryonic stem cells (ESCs) of the inner cell mass into epiblast stem cells. Bottom - *in vitro* differentiation of ESCs into epiblast-like cells (EpiLCs). **B.** Representative images of male wild-type (WT) and *Kdm5c*-KO (5CKO) cells during ESC to EpiLC differentiation. Brightfield images taken at 20X. **C.** No significant difference in primed pluripotency marker expression in wild-type versus *Kdm5c*-KO EpiLCs. Welch's t-test, expression in transcripts per million (TPM). **D.** Number of tissue-enriched differentially expressed genes (DEGs) in *Kdm5c*-KO EpiLCs. * $p < 0.05$, ** $p < 0.01$, *** $p < 0.001$, Fisher's exact test. **E.** Upset plot displaying the overlap of germline DEGs expressed in *Kdm5c*-KO EpiLCs, amygdala (AMY), and hippocampus (HIP) RNA-seq datasets. **F.** UCSC browser view of an example germline gene, *D1Pas1*, that is dysregulated *Kdm5c*-KO EpiLCs (top, purple. Average, $n = 3$), amygdala (middle, red. Average, $n = 4$), and hippocampus (bottom, blue. Average, $n = 4$). **G.** enrichPlot gene ontology analysis comparing enriched biological processes for *Kdm5c*-KO EpiLC, amygdala, and hippocampus germline DEGs. **H.** Top left - Example germline identity DEGs unique to EpiLCs. Top right - Example 2-cell genes that are not dysregulated in *Kdm5c*-KO EpiLCs. p-values for Welch's t-test. Bottom - UCSC browser view of *Dazl* and *Stra8* expression in wild-type and *Kdm5c*-KO EpiLCs (Average, $n = 3$).

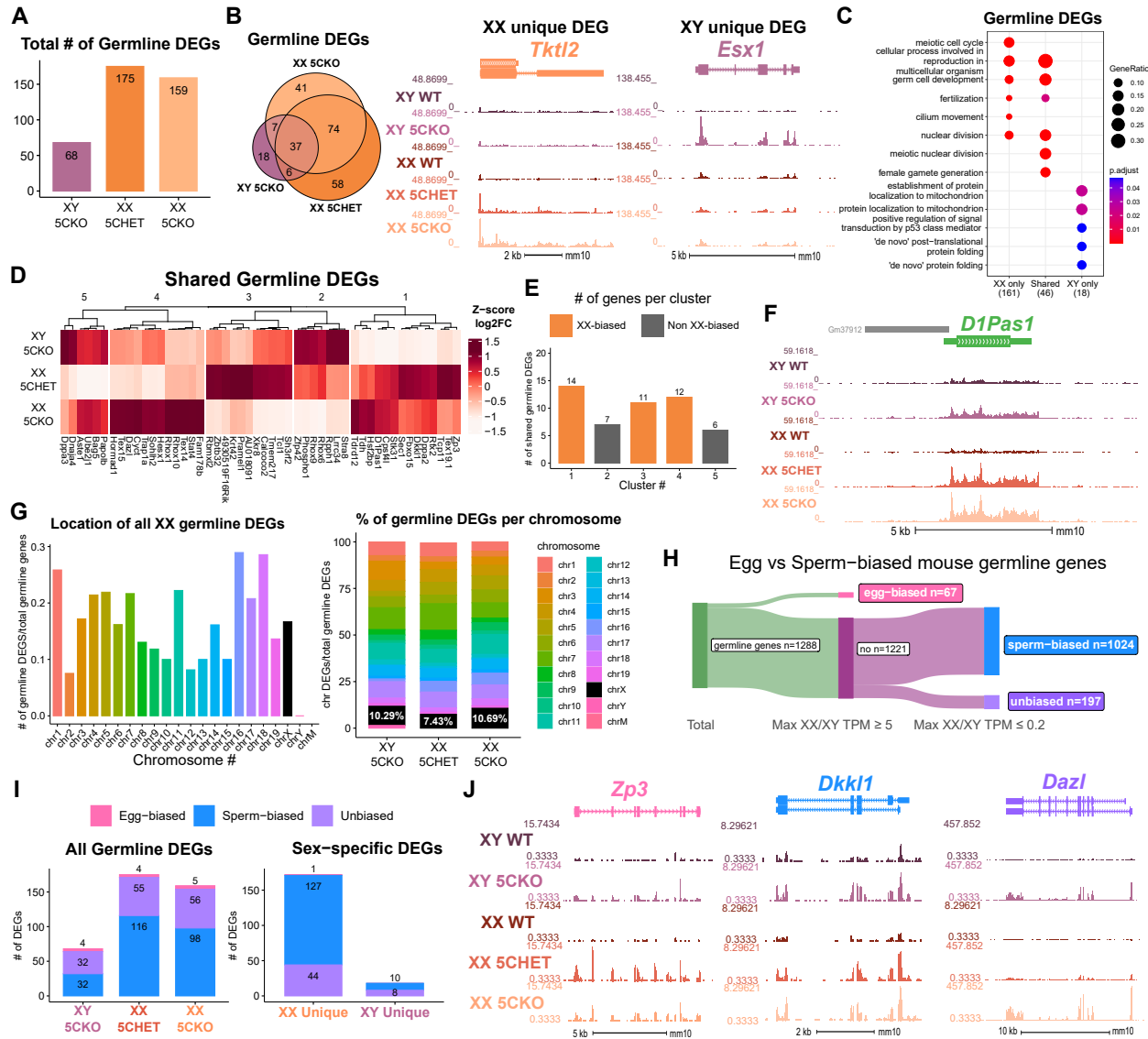


Figure 4: Chromosomal sex influences *Kdm5c*-KO germline gene misexpression. **A.** Total number of germline-enriched RNA-seq DEGs for male hemizygous *Kdm5c* knockout EpilCs (XY 5CKO, purple), female heterozygous *Kdm5c* knockout (XX 5CHET, orange), female homozygous *Kdm5c* knockout (XX 5CKO, light orange) EpilCs. **B.** Left - Eulerr overlap of *Kdm5c* mutant male and female EpilC germline DEGs. Right - Example of germline DEGs unique to females or males, *Tktl2* and *Esx1*. **C.** enrichPlot gene ontology analysis comparing enriched biological processes for germline DEGs shared between *Kdm5c* mutant males and females, or unique to one sex (XX only or XY only). **D.** Heatmap of germline DEGs shared between male and female mutants. Color is the average log 2 fold change from sex-matched wild-type. **E.** Number of genes within each cluster from D. Clusters with higher expression in females compared to males (XX-biased) highlighted in orange. **F.** UCSC browser view of a male and female shared germline DEG *D1Pas1* that is more highly expressed in female mutants (Average, n = 3). **G.** Left - Number of all female germline DEGs located on each chromosome over the total number of germline-enriched genes on that chromosome. Right - Percentage of germline DEGs that lie on each chromosome for each *Kdm5c* mutant. X chromosome highlighted in black. **H.** Sankey diagram classifying egg-biased (pink) and sperm-biased (blue) and unbiased (purple) mouse germline-enriched genes. **I.** Number of egg, sperm, or unbiased germline DEGs for male and female *Kdm5c* mutants. **J.** Example bigwigs of egg-biased (*Zp3*), sperm-biased (*Dkk1*), and unbiased (*Dazl*) germline genes dysregulated in both male and female *Kdm5c* mutants.

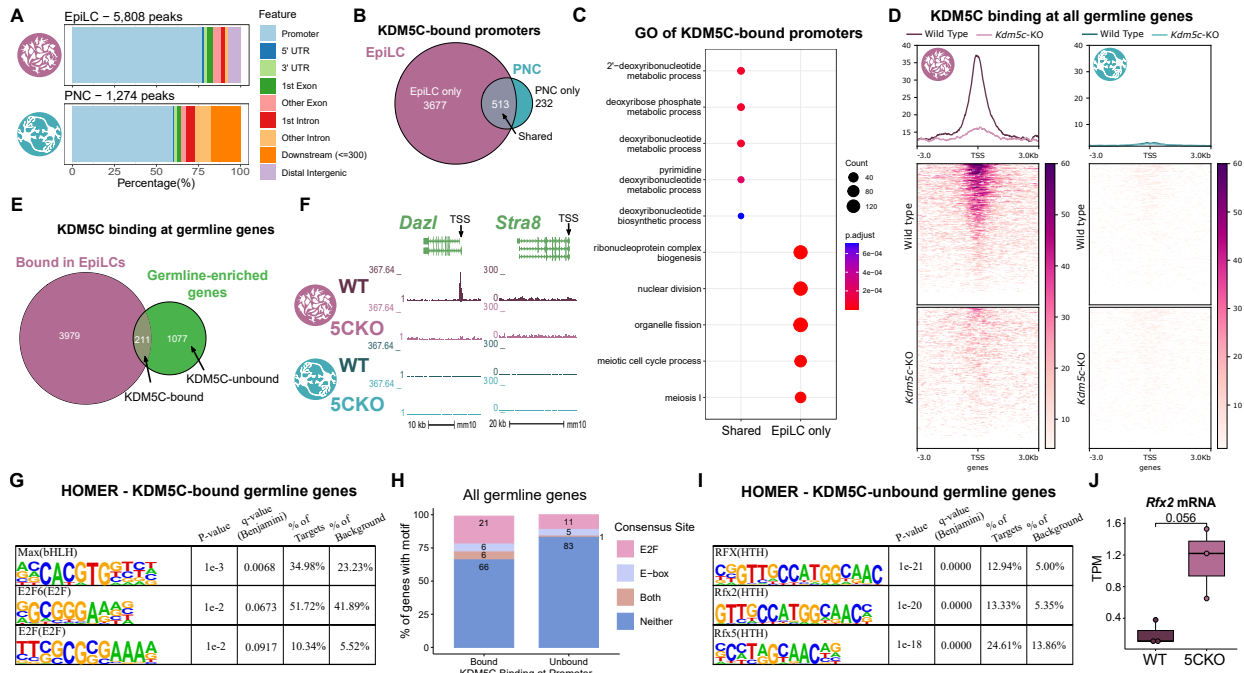


Figure 5: KDM5C binds to a subset of germline gene promoters during early embryogenesis. **A.** ChIPseeker localization of KDM5C peaks at different genomic regions in EpiLCs (top) and hippocampal and cortex primary neuron cultures (PNCs, bottom). **B.** Overlap of genes with KDM5C bound to their promoters ($TSS \pm 500$) in EpiLCs (purple) and PNCs (blue). **C.** Gene ontology (GO) comparison of genes with KDM5C bound to their promoter in EpiLCs and PNCs. Genes were classified as either bound in EpiLCs only (EpiLC only), unique to PNCs (PNC only, no significant ontologies) or bound in both PNCs and EpiLCs (Shared). **D.** Average KDM5C binding around the transcription start site (TSS) of all germline-enriched genes in EpiLCs (left) and PNCs (right). **E.** Eulerr overlap of germline-enriched genes (green) with significant KDM5C binding at their promoter in EpiLCs (purple). **F.** Example KDM5C ChIP-seq signal around the *Dazl* TSS but not *Stra8* in EpiLCs. **G.** HOMER motif analysis of all KDM5C-bound germline gene promoters, highlighting significant enrichment of MAX, E2F6, and E2F motifs. **H.** Number of all gene promoters bound or unbound by KDM5C with instances of the E2F or E-box consensus sequence. **I.** HOMER motif analysis of all KDM5C-unbound germline gene promoters, highlighting significant enrichment of RFX family transcription factor motifs. **J.** Expression of RNA-seq DEG *Rfx2* in wild-type and *Kdm5c*-KO EpiLCs. P-value of Welch's t-test, expression in transcripts per million (TPM).

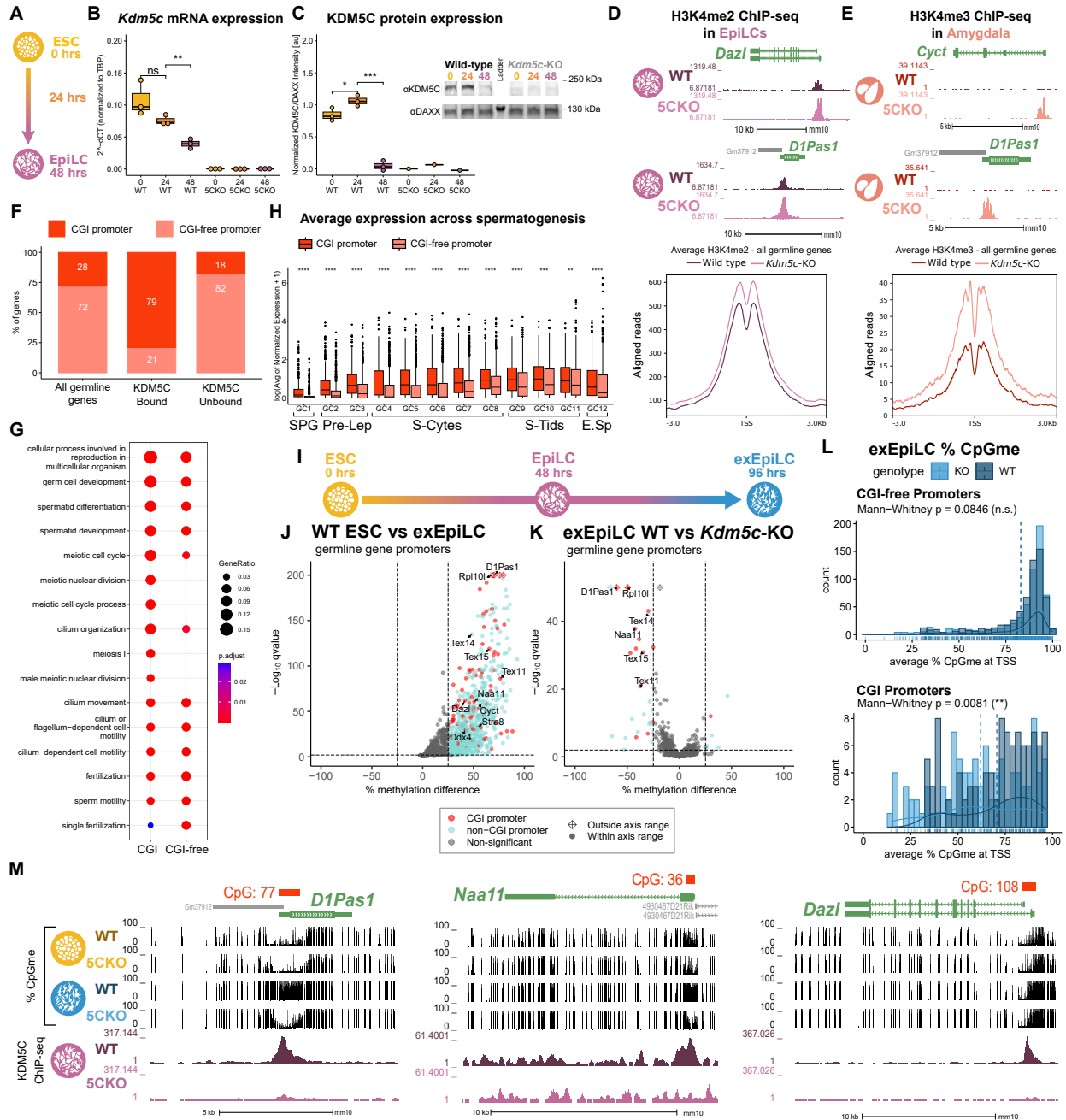


Figure 6: KDM5C promotes long-term silencing of germline genes via DNA methylation at CpG islands. **A.** Diagram of embryonic stem cell (ESC) to epiblast-like cell (EpiLC) differentiation and collection time points. **B.** Real time quantitative PCR (RT-qPCR) of *Kdm5c* mRNA expression in wild-type (WT) and *Kdm5c*-KO (5CKO) ESCs at 0, 24, and 48 hours of differentiation into EpiLCs. Expression calculated in comparison to TBP mRNA expression ($2^{-\Delta\Delta CT}$). * $p < 0.05$, ** $p < 0.01$, *** $p < 0.001$, Welch's t-test. **C.** KDM5C protein expression normalized to DAXX. Quantified intensity using ImageJ (artificial units - au). Right - representative lanes of Western blot for KDM5C and DAXX. * $p < 0.05$, ** $p < 0.01$, *** $p < 0.001$, Welch's t-test. **D.** Top - Representative UCSC browser view of histone 3 lysine 4 dimethylation (H3K4me2) ChIP-seq signal at two germline genes in wild-type and *Kdm5c*-KO EpiLCs. Bottom - Average H3K4me2 signal at the TSS of all germline-enriched genes in wild-type (dark purple) and *Kdm5c*-KO (light purple) EpiLCs. **E.** Top - Representative UCSC browser view of histone 3 lysine 4 trimethylation (H3K4me3) ChIP-seq signal at two germline genes in the wild-type (WT) and *Kdm5c*-KO (5CKO) adult amygdala. Bottom - Average H3K4me3 signal at the transcription start site (TSS) of all germline-enriched genes in wild-type (dark red) and *Kdm5c*-KO (light red) amygdala. **F.** Percentage of germline genes that harbor CpG islands (CGIs) in their promoters (CGI promoter, red), based on UCSC annotation. Left - percentage of all germline-enriched genes, middle - KDM5C-bound germline genes, and right - KDM5C-unbound germline genes. (Legend continued on next page.)

Figure 6: KDM5C promotes long-term silencing of germline genes via DNA methylation at CpG islands. (Legend continued.) **G.** enrichPlot gene ontology analysis of germline genes with (CGI-promoter) or without (CGI-free) CGIs in their promoter. **H.** Expression of germline genes with (CGI-promoter, red) or without (CGI-free, salmon) CGIs in their promoter across stages of spermatogenesis from Green et al 2018. SPG - spermatogonia, Pre-Lep - preleptotene spermatocytes, S-Cytes - meiotic spermatocytes, S-Tids - post-meiotic haploid round spermatids, E.Sp - elongating spermatids. Wilcoxon test, * $p < 0.05$, ** $p < 0.01$, *** $p < 0.001$, **** $p < 0.0001$. **I.** Diagram of ESC to extended EpiLC (exEpiLC) differentiation. **J.** Volcano plot of whole genome bisulfite sequencing (WGBS) comparing CpG methylation (CpGme) at germline gene promoters ($TSS \pm 500$) in wild-type (WT) ESCs versus exEpiLCs. Significantly differentially methylated promoters ($q < 0.01$, $|methylated difference| > 25\%$) with CGIs in red, CGI-free promoters in light blue **K.** Volcano plot of WGBS of wild-type (WT) versus *Kdm5c*-KO exEpiLCs for germline gene promoters. Promoters with CGIs in red, CGI-free promoters in light blue. **L.** Histogram of average percent CpGme at the promoter of germline genes with or without CGIs. Wild-type in navy and *Kdm5c*-KO (KO) in light blue. Dashed lines are average methylation for each genotype, p-values for Mann-Whitney U test. **M.** UCSC browser view of germline genes, showing UCSC annotated CGI with number of CpGs, representative CpGme in wild-type (WT) and *Kdm5c*-KO (5CKO) ESCs and exEpiLCs, and KDM5C ChIP-seq signal in EpiLCs.